Earth-Science Reviews
December 2022, Volume 235, Pages 104248 (19p.)
https://doi.org/10.1016/j.earscirev.2022.104248
https://archimer.ifremer.fr/doc/00805/91723/

Effects of plant types on terrestrial leaf wax long-chain n-alkane biomarkers: Implications and paleoapplications

Liu Jinzhao [1, 2, *], Zhao Jiaju [1], He Ding [3], Huang Xianyu [4], Jiang Chong [1], Yan Hong [1], Lin Guanghui [5], An Zhisheng [1]

[1] State key Laboratory of Loess and Quaternary Geology, Institute of Earth Environment, Chinese Academy of Sciences, Xi'an 710061, China
[2] National Observation and Research Station of Earth Critical Zone on the Loess Plateau of Shaanxi, Xi'an, 710061, China
[3] Department of Ocean Science, The Hong Kong University of Science and Technology, Hong Kong 999077, China
[4] State Key Laboratory of Biogeology and Environmental Geology, China University of Geosciences, Wuhan 430074, China
[5] Ministry of Education Key Laboratory for Earth System Modeling, Department of Earth System Science, Tsinghua University, Beijing 100084, China

* Corresponding author : Jinzhao Liu, email address : liujinzhao@ieecas.cn

Abstract :

Terrestrial leaf wax n-alkane biomarkers provide considerable insights into paleoenvironmental reconstruction. Over decades, a substantial number of field investigations were performed to constrain hydroclimatic factors that influence leaf wax n-alkane biomarkers to improve their utility for paleoenvironmental applications. However, a critical issue, the plant type effects, does exist which potentially affects the fidelity of leaf wax n-alkane biomarkers for paleohydroclimate calibration. Here we review the effects of plant types on terrestrial leaf wax n-alkane biomarkers from three aspects: leaf wax n-alkane distribution (wood vs. non-wood), hydrogen isotope (δ2Hwax; dicot vs. monocot) and carbon isotope (δ13Cwax; C3 vs. C4) biomarkers. Then we demonstrate the relationships between three forms of leaf wax n-alkane biomarkers, and provide examples of the cross-calibration among them in paleo-applications. The in-depth review of plant type effects on leaf wax n-alkane biomarkers will be helpful to interpret the hydroclimate and vegetation signals in the geologic past.

Keywords : Leaf wax n-alkane biomarker, Plant type effect, n-Alkane, Hydrogen and carbon isotopes

1. Introduction

Significant advances in compound-specific analytical techniques have facilitated the use of plant lipids as proxies for the reconstruction of paleoenvironment since late 1990s (Huang et al., 1996; Meyers, 2003; Seki et al., 2010; Sessions, 2016; Diefendorf and Freimuth, 2017). Leaf wax *n*-alkane biomarkers were developed as a powerful tool for paleoenvironmental reconstruction. Of these biomarkers, the long-chain *n*-alkanes of leaf wax are the most commonly used because they possess many advantages: 1) a ubiquitous distribution in ancient sedimentary archives that originates from epicuticular waxes of vascular higher plants (Eglinton and Hamilton, 1967), 2) the relatively high stability that is resistant to microbial degradation (Bush and McInerney, 2013), 3) a simple extraction from diverse matrices using well-established biochemical approaches (Eglinton and Hamilton, 1963; Ardenghi et al., 2017), and 4) an excellent preservation of the original isotopic composition after burial (Polissar et al., 2009) otherwise significant alteration by microorganisms at certain conditions (Brittingham et al., 2017).

Numerous approaches were developed to quantify molecular distributions of long-chain *n*-alkanes in plants, soils, and sediments and extract information about past changes in environmental conditions (Cranwell, 1973; Bush and McInerney, 2013; Freimuth et al., 2019). Long-chain *n*-alkane distributions can be characterized by various *n*-alkane indices, such as the carbon number range (C_{range}), carbon number

maximum (C_{max}), carbon preference index (CPI), ratios of different *n*-alkanes, percent of aquatic plants (P_{aq}) and average chain length (ACL). The *n*-alkane C_{range} is mainly concentrated on the range of C_{21}-C_{35}, with the C_{max} of C_{27}, C_{29}, C_{31}, or C_{33} in modern plants (Wang and Liu, 2012; Carr et al., 2014; Badewien et al., 2015; Liu et al., 2018). The *n*-alkane distributions exhibit a strong odd-over-even predominance, which is reflected in the CPI values (Eglinton and Hamilton, 1967). In particular, the CPI is used to indicate terrestrial plant sources and thermal immaturity of source rock, with generally greater than one for terrestrial plants (Eglinton and Hamilton, 1967; Kuhn et al., 2010; Bush and McInerney, 2013). The ACL values are associated with plant types such that C_{31} predominates in grasses (monocots), while the C_{27} and C_{29} predominate in trees and shrubs (dicots) in higher plants (Cranwell, 1984; Meyers, 2003; Duan et al., 2011a; Wang et al., 2018). However, the ACL indicator was likely robust locally and regionally, but would not globally (Bush and McInerney, 2013). In lacustrine environment, the P_{aq} has been proposed for distinguishing terrestrial and aquatic sources because the long-chain *n*-alkanes are usually more abundant in terrestrial plants than in aquatic plants (Ficken et al., 2000; Wang and Liu, 2012; Wang et al., 2018).

Stable hydrogen and carbon isotopes of leaf wax *n*-alkanes (δ^2H_{wax} and $\delta^{13}C_{wax}$) showed wide applications in paleoenvironmental studies (Pagani et al., 2006; Schefuβ et al., 2011; Feakins et al., 2012; Niedermeyer et al., 2014; Nieto-Moreno et al., 2016; Liu and An, 2020; Wang et al., 2021). The applications of δ^2H_{wax} values substantially

depend on a significant positive correlation between δ^2H_{wax} values in various archives (e.g., plants, soils, lake and marine sediments) and precipitation δ^2H at scales ranging from local, regional to global scales (Liu and Yang, 2008; Sachse et al., 2012; Collins et al., 2013; Feakins et al., 2016a; Liu and An, 2018; Hou et al., 2018). However, δ^2H_{wax} values are also affected by plant types (dicots versus monocots; Liu et al., 2016) and ecosystem evapotranspiration from leaves and soils (Feakins and Sessions, 2010a; Kahmen et al., 2013a, b). Additionally, the biosynthesis for δ^2H_{wax} values combines a series of biochemical processes modulated by climate (e.g., relative humidity and temperature) and ecology (e.g., plant types etc.) (Sachse et al., 2012; Newberry et al., 2015; Zhang et al., 2017; Cormier et al., 2018) although these processes are not understood. On the other hand, theoretical and empirical studies showed that $\delta^{13}C_{wax}$ values are sensitive to bioclimatic variables, such as temperature, water availability, concentrations of CO_2 and vegetation types (Diefendorf et al., 2010; Cernusak et al., 2013; Wu et al., 2017; Diefendorf and Freimuth, 2017). Among these variables, it is well established that $\delta^{13}C_{wax}$ values in higher plants are strongly affected by carbon fixation pathways (C_3 versus C_4) during photosynthesis in terrestrial higher plants (Rieley et al., 1991; Collister et al., 1994; Chikaraishi and Naraoka, 2003; Ankit et al., 2017; Liu and An, 2020). Collectively, both δ^2H_{wax} and $\delta^{13}C_{wax}$ values have been interpreted as indicators of hydroclimatic variables and vegetation changes (He et al., 2016; Liu and An, 2018, 2020).

Leaf wax *n*-alkane biomarkers mainly contain three forms of information, including

n-alkane distribution, δ^2H_{wax} and $\delta^{13}C_{wax}$ values. Grown under the same environmental conditions with the use of the same source water (i.e., soil and leaf water) and atmospheric CO_2, the δ^2H_{wax} and $\delta^{13}C_{wax}$ values differ substantially among plant types (Chikaraishi and Naraoka, 2003; Liu et al., 2006; Hou et al., 2007; Sachse et al., 2012; Ankit et al., 2017; Liu and An, 2020). Over the last decade, several reviews have focused on an alternative proxy of *n*-alkane distribution (Bush and McInerney, 2013), δ^2H_{wax} (Sachse et al., 2012; Sessions, 2016; Liu and An, 2019) or $\delta^{13}C_{wax}$ values (Diefendorf and Freimuth, 2017; Liu and An, 2020), we do this review by analyzing the effects of plant types on leaf wax *n*-alkane biomarkers involved all three aspects in terrestrial higher plants, and demonstrate the relationships and cross-calibrations between them, and their paleo-applications in sediments.

2. Methods

The three updated global datasets were compiled for three forms of leaf wax *n*-alkane biomarkers based upon the previously published datasets in this review (Fig. 1; see Datasets). The long-chain *n*-alkanes (> C_{19}) in terrestrial higher plants was expanded to a larger new dataset (n = 3538) from a prior global dataset of Bush and McInerney (n = 1596), in which we complemented the geographical (e.g., latitude, longitude, altitude) and biological (e.g., plant type, wood vs. non-wood) information and removed the species of aquatic plants, mosses, succulents, etc. Likewise, the δ^2H_{wax} and $\delta^{13}C_{wax}$ datasets were updated through supplementing the recently published data based upon our previous datasets (δ^2H_{wax} dataset from Liu and An, 2019 and $\delta^{13}C_{wax}$

dataset from Liu and An, 2020). The *n*-alkane indices (i.e., C_{max}, ACL and CPI) were calculated to characterize the terrestrial *n*-alkane distribution. Additionally, the isotopes of C_{29} *n*-alkane of leaf wax were selected as the representative of δ^2H_{wax} and $\delta^{13}C_{wax}$ values because the *n*-C_{29} is abundant across plant types and highly coherent among the most long-chain *n*-alkanes (*n*-C_{27}, *n*-C_{29}, *n*-C_{31}) in terrestrial plants (Feakins et al., 2018; Liu and An, 2020).

Pearson correlation was conducted to describe various correlations between leaf wax *n*-alkane biomarkers (δ^2H_{wax} and $\delta^{13}C_{wax}$) and relevant variables. A one-way ANOVA combined with a *post hoc* Tukey's test was performed to identify the significant differences among plant life forms (e.g. tree, shrub, herb , forb, grass, sedge) and plant types (e.g., dicot, monocot, gymnosperm, magnoliid), and independent-sample's *t*-tests were used to identify differences between two groups. If site location (latitude and longitude) and altitude were stated in the publications, these data were used directly; otherwise they were determined using Google Earth and the sites provided in the original publications. We checked each species by using Web search engines such as Google and Baidu to determine the family, plant type, photosynthetic pathway, and plant life form. We classified each site in the global datasets into one of five subsets: tropical, temperate, arid, cold, and polar zones based on the local Köppen–Geiger climate classification (Kottek et al., 2006). Digital maps of the global distribution of Köppen–Geiger climate classes were available at http://koeppen-geiger.vu-wien.ac.at.

3. Effect of plant types on leaf wax *n*-alkane distributions

Local-scale surveys of leaf wax *n*-alkanes in modern plants indicate that the *n*-alkane concentration and distribution vary among plant species at local scales (Polissar and Freeman, 2010; Bush and McInerney, 2013; Diefendorf et al., 2015). Long chain *n*-alkane concentration is typically higher in angiosperm trees and shrubs than many gymnosperms, more specifically, conifers (Diefendorf and Freimuth, 2017). In addition to woody angiosperms, other life forms such as grasses, succulents, herbs, and ferns produce significant concentrations of leaf waxes (Rommerskirchen et al., 2006; Bush and McInerney, 2013). Moreover, leaf wax *n*-alkane distributions were demonstrated to vary with environmental conditions (Schefuβ et al., 2003; Vogts et al., 2012; Bush and McInerney, 2015; Howard et al., 2018) and plant types (Rommerskirchen et al., 2006; Garcin et al., 2014; Diefendorf et al., 2015).

Our updated global *n*-alkane dataset shows the average long-chain *n*-alkane distributions across life forms (Fig. 2a), plant types (Fig. 2b), and wood vs. non-wood (Fig. 2c). The C_{29} and C_{31} *n*-alkanes are the relatively highest abundances in different plant classifications (Fig. 2), which is supported by the previous observations at local/regional (Ficken et al., 2000; Meyers, 2003; Kuhn et al., 2010; Luo et al., 2012; Badewien et al., 2015; Liu et al., 2018) and global scales (Bush and McInerney, 2013). There are significant differences in the terrestrial leaf wax *n*-alkane indices such as ACL, CPI, $C_{29}/(C_{29} + C_{31})$, and $(C_{27} + C_{29})/(C_{27} + C_{29} + C_{31} + C_{33})$ among life forms (Fig. 3a, b, c, d), taxonomic lineages (Fig. 3e, f, g, h), and wood vs. non-wood (I, j, k,

l) although the differences do not seem to be large enough for distinguishing plant classifications at the global scale. The result is consistent with the prior global *n*-alkane analysis that it was hard to make chemotaxonomic distinction only by using *n*-alkane abundances at the global scale (Bush and McInerney, 2013). However, the differences in *n*-alkane distributions (e.g., ACL and CPI) between woods (tree and shrub) and non-woods (herb, forb, grass, sedge) will become more distinguished when the global data is grouped based on the climate zones or across the latitude/longitude gradient (Fig. 4; Supplementary Table S1). There are significant differences in the ACL and CPI between wood and non-wood across five climate zones ($p < 0.01$ or $p < 0.05$), except the ACL in the polar zone ($p = 0.13$; Fig. 4). The ACL in non-woods is a bit higher than that in woods, but the CPI shows opposite patterns between woods and non-woods at each climate zones (Supplementary Table S1; Fig. 4). Meanwhile, the ACL appears to be higher in warm zones (e.g., Tropical, Temperate) than that in cold zones (e.g., Cold, Polar), but the CPI does not (Supplementary Table S1). At the global scale, such significant differences between woods and non-woods are also observed by a majority of the results across latitude and longitude gradients, but the global differences in the ACL (29.9±1.2 and 30.0±1.1 for wood and non-wood, respectively) and CPI (14.1±14.5 and 9.6±11.5 for wood and non-wood, respectively) appeared to be insignificant (Fig. 4; Supplementary Table S1). Thus, there is a relatively significant difference in *n*-alkane distribution (i.e., ACL, CPI) between woods and non-woods across climate zones but it becomes weakened at the global scale, probably due to the mask of mixture of climate zones. The *n*-alkane distribution

biomarker to distinguish plant classifications are relatively robust when the scale is restricted at the local and regional level.

Some local/regional calibration studies interpreted leaf wax *n*-alkane distributions as a paleoclimatic proxy from sediment cores (Rommerskirchen et al., 2006; Schouten et al., 2007; Tipple and Pagani, 2013), showing that the ACL was correlated with temperature (Sachse et al., 2006; Tipple and Pagani, 2013), relative humidity and aridity (Hoffmann et al., 2013) and vapor pressure deficit (VPD; Eley and Hren, 2018) although the temperature did not, at a global scale, appear to exert significant control on ACL, likely because of differences in ACL among plant groupings (Fig. 3a, e, i; Diefendorf and Freimuth, 2017). Similar to the ACL, the difference in CPI is also significant among plant groupings (Fig. 3b, f, j), but the values span a large range with relatively higher CPI values in woods than non-woods (Fig. 3j). Importantly, angiosperms (dicot, monocot, magnoliid) have significantly higher average CPI value than gymnosperms (Fig. 3l). These results are consistent with the observations of Bush and McInerney (2013). Additionally, the long-chain *n*-alkane ratios, e.g., $C_{29}/(C_{29} + C_{31})$, $(C_{27} + C_{29})/(C_{27} + C_{29} + C_{31} + C_{33})$, vary significantly with plant groupings (Fig. 3c, g, k, d, h, l), with relatively higher values in woods (tree and shrub; dicot and magnoliid) relative to non-woods (herb, forb, grass; monocot) because the C_{max} value arose at C_{27} or C_{29} in woody plants (trees and shrubs) whereas that occurs at C_{31} or C_{33} in grasses (See Datasets *n*-alkanes). These results were supported by many observations at local and regional scales (Cranwell, 1984; Meyers, 2003; Krull

et al., 2006; Rommerskirchen et al., 2006; Vogts et al., 2009; Garcin et al., 2014; Liu et al., 2018).

In summary, the long-chain *n*-alkane distributions carries both vegetation and hydroclimate signals in terrestrial higher plants, the *n*-alkane indices such as ACL, CPI, $C_{29}/(C_{29} + C_{31})$, and $(C_{27} + C_{29})/(C_{27} + C_{29} + C_{31} + C_{33})$ can be used to distinguish plant groupings when climate change is constrained at local/regional scales (Fig. 4). However, it can be weak to assess the extent to which variation is driven by plant adaptation to environmental surroundings and/or chemotaxonomic patterns, especially at the global scale (Bush and McInerney, 2013) because of the conflation of hydroclimatic conditions and vegetation changes. These combined signals of vegetation and hydroclimate in terrestrial higher plants are well preserved in natural archives such as soils, peats, and sediments (Rommerskirchen et al., 2006; Bush and McInerney, 2015). Leaf wax *n*-alkane distributions are likely useful in combination with other proxy data, in which situation leaf wax *n*-alkane distributions can be envisaged to reflect vegetation and/or hydroclimate changes. For example, significant shifts in leaf wax *n*-alkane distributions with plant types are secondarily helpful in interpretation of δ^2H_{wax} and $\delta^{13}C_{wax}$ records in local sediments (Feakins and Sessions, 2010a; Sachse et al., 2012; Zhuang et al., 2014; Wang et al., 2021). Simultaneously, leaf wax *n*-alkane biomarker poses challenges when interpreting *n*-alkane distribution in sediments because scaling relationships have not been developed between local, regional, continental, and global scales. In future research, it

needs to construct a scale criterion at which leaf wax *n*-alkane biomarker can be used to distinguish between plant groupings.

4. Effect of plant types on δ^2H_{wax} values

The history evolution shows the effect of plant types on δ^2H_{wax} values in modern plants, especially at scale transitions (Fig. 5). In analogy with the classification on carbon isotopes in modern plants, Chikaraishi and Naraoka (2003) investigated plant-level δ^2H_{wax} values in Japan and Thailand, and proposed that C_4 plants had relatively lower δ^2H_{wax} values than C_3 plants in terrestrial plants. However, Liu et al. (2006) found that most of the C_3 plants were trees and shrubs, whereas the C_4 plants were from the Gramineae in the plants recorded by Chikaraishi and Naraoka (2003). They proposed that plant life forms (woods vs. grasses) played a dominant role in determining δ^2H_{wax} values in terrestrial plants, instead of photosynthetic pathways. Subsequently, the consistent results were observed at a catchment in south-central Massachusetts, USA (Hou et al., 2007) and over the global scale (Liu and Yang, 2008; Sachse et al., 2012). Applying the global dataset, we found most of the herbaceous plants (mainly forbs and herbs) with higher δ^2H_{wax} values in Liu and Yang (2008)'s dataset that belongs to dicot plants (Liu et al., 2016). When regrouped their previous outliers based on plant taxonomy (dicots vs. monocots) rather than plant life forms, we observed distinguished distribution patterns in δ^2H_{wax} values between dicots and monocots (Liu et al., 2016). To further confirm our updated classification that controls on δ^2H_{wax} values, we sampled a variety of modern plants in the Qiushui catchment on

the Chinese Loess Plateau, and found that δ^2H_{wax} values in dicots were significantly ^{2}H-enriched relative to those in monocots, especially for non-woody dicots (Liu et al., 2017). These results were also supported by various observations ranging from local to global scales (Daniels et al., 2017; Zhang et al., 2017; Pedentchouk and Zhou, 2018; Liu and An, 2019; He et al., 2020; Bai et al., 2020). So far, the plant type (dicots vs. monocots) is the well-recognized classification that exerts a critical role in determining δ^2H_{wax} values in modern plants, and thus the effect of plant types on δ^2H_{wax} values persists from the catchment-level to global scale.

Our expanded global dataset shows that the δ^2H_{wax} values in both dicots and monocots decrease significantly from Tropical to Polar zone, which is consistent with the trend of δ^2H_{wax} vs. latitude (Supplementary Table S2; Liu and Yang, 2008; Liu et al., 2016; Liu and An, 2019). There are significant differences in δ^2H_{wax} values between dicots and monocots, which persist at high-level significances across climate zones ($p < 0.001$ or $p < 0.05$; Fig. 6). It is reliably robust for our updated classification (dicots vs. monocots) that controls on δ^2H_{wax} values from local, catchment, regional to global scales. Globally, dicots tend to be isotopically ^{2}H-enriched (~ 30‰) relative to monocots, with the global mean δ^2H_{wax} values of -173 ± 36‰ for dicots and -195 ± 32‰ for monocots (Fig. 7). This is consistent with previously plant-derived values at the global scale (Liu and Yang, 2008; Sachse et al., 2012; Liu et al., 2016; Liu and An, 2019). Locally, the difference in δ^2H_{wax} values become more obvious, with -164 ± 15‰ and -193 ± 16‰ for dicots and monocots on Chinese Loess Plateau, respectively (Liu

et al., 2017) and -224 ± 7‰ and -302 ± 8‰ for dicots and monocots in the Alaskan Arctic tundra, respectively (Daniels et al., 2017). Generally, dicots are ^{2}H-enriched compared to monocots, but both of which decrease significantly with the increase of latitudes (Liu and An, 2019). What is the underlying mechanism for the difference in $\delta^{2}H_{wax}$ values between dicots and monocots? A fundamental difference between dicots and monocots is the veinal architecture of leaves, with dicots having a reticulate veinal architecture whereas monocot leaves having parallel veins (Helliker and Ehleringer, 2000). The difference of veinal architecture between dicots and monocots leads to intra-leaf hydrogen isotopic gradients of leaf water, which is supported by oxygen isotopic variations of leaf water and cellulose between dicots and monocots (Helliker and Ehleinger, 2002; Farquhar and Gan, 2003; Barbour, 2007; Song et al., 2013). Fortunately, our recent investigation of segmented leaf samples between dicots and monocots indicates that leaf water isotopic gradients can be well recorded in intra-leaf $\delta^{2}H_{wax}$ heterogeneity, associated with the veinal difference between dicots and monocots (Liu et al., 2021). Thus, the underlying mechanism for the difference in $\delta^{2}H_{wax}$ values between dicots and monocots derive probably from different biosynthetic fractionations (Liu et al., 2016), which is in fact underpinned by the intra-leaf variations of $\delta^{2}H_{wax}$ values between dicots and monocots.

The $\delta^{2}H_{wax}$ values increase with the increase of precipitation $\delta^{2}H$ values ($\delta^{2}H_{p}$) in terrestrial plants, following approximate slopes in both dicots and monocots (Fig. 7a). The approximate slopes further support our finding that the plant type (dicots vs.

monocots) plays an important role in determining δ^2H_{wax} values in terrestrial plants (Fig. 7b). Significant positive correlations between δ^2H_{wax} and δ^2H_p values are observed in dicots ($R^2 = 0.50$, $p < 0.01$) and monocots ($R^2 = 0.35$, $p < 0.01$), but no or weak correlations occur in apparent fractionation (ε_{app}) with δ^2H_p values in dicots ($R^2 = 0.09$, $p < 0.01$) or monocots ($R^2 = 0.02$, $p = 0.02$) (Fig. 7c). These results indicate that δ^2H_p values conduct a key control on δ^2H_{wax} values (Liu and Yang, 2008; Sachse et al., 2012; Liu and An, 2019), but not on ε_{app} values (Hou et al., 2008; Daniels et al., 2017; Zhang et al., 2017; Liu and An, 2019). The global independence of ε_{app} values is consistent with previous studies conducted on local and regional samples (Tipple and Pagani, 2013; Garcin et al., 2012; Daniels et al., 2017; Liu and Liu, 2019). The ε_{app} values vary significantly with climate zones within dicots ($p < 0.001$) and monocots ($p < 0.001$) (Supplementary Table S2). The global average ε_{app} values are -107 ± 28.5‰ and -142 ± 28.5‰ for dicots and monocots, respectively (Fig. 7d; Liu and An, 2019), with monocots ^{2}H-depleted by 35‰ relative to dicots (Supplementary Table S2). Such differences in ε_{app} values between dicots and monocots persist steadily across climate zones although the large standard deviations (S.D.) exist (Supplementary Table S2). The ε_{app} values incorporate the influences of soil evaporation, plant transpiration, and biosynthesis processes (Sachse et al., 2012; Liu and An, 2018). Both soil evaporation and leaf transpiration controlled by hydroclimatic factors lead to ^{2}H-enrichment relative to precipitation (Feakins and Sessions, 2010a; Kahmen et al., 2013a, b), which offsets the negative fractionation associated with leaf wax *n*-alkane biosynthesis (Sessions et al., 1999; Cormier et al., 2018). These processes

synergistically results in steady, or less-varied ε_{app} values (Smith and Freeman, 2006; Hou et al., 2008; Zhang et al., 2017; Daniels et al., 2017; Liu and An, 2019). A series of evidences in support of steady ε_{app} values are as a result of the regulation of leaf water ^{2}H-enrichment by restricting their water loss especially in arid conditions (Feakins and Sessions, 2010a), changes between vegetation types and relative humidity (Hou et al., 2008), the counteraction of soil evaporation and biosynthesis (Zhang et al., 2017), and the offset of dicots and monocots across latitudes (Liu and An, 2019). In addition, the $\delta^{2}H_{wax}$ and ε_{app} values in gymnosperms are similar to those in dicots (Liu et al., 2016; Liu and An, 2019), so dicots can be used as a representative of gymnosperms for comparisons in this study. The reader is referred to the extensive investigation of gymnosperms by Liu et al. (2016) and Liu and An (2019).

5. Effect of plant types on $\delta^{13}C_{wax}$ values

Numerous studies have shown that $\delta^{13}C_{wax}$ values were influenced by both geo-environmental factors (e.g., water availability, temperature, light intensity, aridity, altitude; Farquhar et al., 1989; Diefendorf et al., 2010; Schubert and Jahren, 2012; Vogts et al., 2009; Wu et al., 2017) and biochemical factors (e.g., photosynthetic pathways, plant types; Cernusak et al., 2013; Diefendorf and Freimuth, 2017). The photosynthetic pathway is the largest of these factors, with biomass produced by plants using C_3 carbon fixation pathway (Calvin-Benson) significantly ^{13}C-depleted relative to waxes produced by the C_4 carbon fixation pathway (Hatch-Slack) (O'Leary, 1981; Collister et al., 1994; Collatz et al., 1998). The third photosynthetic pathway,

Crassulacean acid metabolism (CAM), is not included in this study because these plants only contribute to about 7% of vascular plants (Boom et al., 2014). There were significant variations in $\delta^{13}C_{wax}$ values among photosynthetic pathways and plant types, with typically ranging from -28‰ to -43‰ in the C_3 plants (including dicots, monocots, gymnosperms, and magnoliids), while from -17‰ to -27‰ in the C_4 monocots at the family level (Fig. 8). These results were consistent with the ranges of previous studies (Rieley et al., 1991; Collister et al., 1994; Chikaraishi and Naraoka, 2003; Bi et al., 2005; Ankit et al., 2017). The global mean values were -35.0±3.2 and -21.9±2.4 for C_3 and C_4 plants, respectively (Fig. 9), such differences in $\delta^{13}C_{wax}$ values between C_3 and C_4 plants were persistent remarkably across climate zones, except the polar zone because of the lack of C_4 plants available in our dataset ($p < 0.001$; Fig. 9; Supplementary Table S3). In addition, there were significant differences in $\delta^{13}C_{wax}$ values for C_3 ($p < 0.01$) and C_4 plants ($p < 0.05$) across climate zones (Supplementary Table S3). Therefore, the difference in $\delta^{13}C_{wax}$ values can be used to classify plants into C_3 and C_4 groupings (DeNiro and Epstein, 1977).

Our meta-analysis indicates different responses of $\delta^{13}C_{wax}$ values between C_3 and C_4 plants to MAP and MAT over the globe (Liu and An, 2020). A significant negative correlation between $\delta^{13}C_{wax}$ values and MAP in C_3 plants compared with C_4 plants exists, while a significant positive correlation between $\delta^{13}C_{wax}$ values and MAP in C_4 plants relative to C_3 plants occurs (Fig. 10a, b). The observation is consistent with the result of bulk $\delta^{13}C$ values in modern plants (Rao et al., 2017). Diefendorf et al. (2010)

identified the MAP as the strongest control on bulk $\delta^{13}C$ values compared to other geo-climate factors, consistent with the result by Kohn (2010). However, C_4 plants yield a closer correlation with temperature than C_3 plants because C_4 plants have a competitive growth advantage over C_3 plants in conditions of high temperature, aridity and low atmospheric CO_2 concentration (Edwards et al., 1985; Farquhar et al., 1989; Sage et al., 1999). The mechanism underlying the contrasting responses of $\delta^{13}C_{wax}$ values between C_3 and C_4 plants to precipitation and temperature is associated with the carbon isotope discrimination against ^{13}C during photosynthesis (Fig. 10c; Farquhar et al., 1989). The carbon isotope fractionation between C_3 and C_4 plants contains kinetic discrimination factors associated with diffusion in air through the stoma (denoted by *a*) and enzyme fraction (denoted by *b*) associated with carboxylation during photosynthesis, as well as the ratio of the CO_2 concentration in the internal stomatal cavity (C_i) and the atmosphere (C_a). The expression for C_3 plants (Farquhar et al., 1982) is,

$$\delta^{13}C_3 = \delta^{13}C_{air} - a_3 - (b_3 - a_3)\frac{C_i}{C_a}$$

while the expression for C_4 plants (Farquhar and Richards, 1984) is,

$$\delta^{13}C_4 = \delta^{13}C_{air} - a_3 - (b_4 + b_3 \times f - a_3)\frac{C_i}{C_a}$$

where $\delta^{13}C_3$ and $\delta^{13}C_4$ represent $\delta^{13}C_{wax}$ values for C_3 and C_4 plants, respectively, and $\delta^{13}C_{air}$ indicates the $\delta^{13}C$ values in ambient atmosphere. The ratio of C_i/C_a in both expressions is a key value that primarily reflects the stomatal conductance of plant leaves. The significant difference between C_3 and C_4 plants is that the term *b* in C_3 plants is only reflected by b_3 caused by Rubisco carboxylation, while it is replaced

by $(b_4 + b_3 \times f)$ in C_4 plants that are associated with Rubisco and PEP carboxylase. In C_3 plants, the coefficient of C_i/C_a (i.e., $b_3 - a_3$) is not equal to zero, but in C_4 plants, the term $(b_4 + b_3 \times f - a_3)$ is often close to zero with ^{13}C discrimination responding little to variation in C_i/C_a (Evans et al., 1986; Farquhar et al., 1988). It is thus reasonable that $\delta^{13}C_{wax}$ values are correlated with the ratio of C_i/C_a, associated with water availability (Farquhar et al., 1989), but not in C_4 plants. The expression in C_4 plants can be simplified as $\delta^{13}C_4 = \delta^{13}C_{air} - a_3$, which is strongly affected by temperature associated with a positive correlation between MAP and MAT at the global scale (Rao et al., 2017). Overall, $\delta^{13}C_{wax}$ values in C_3 plants appear to be mainly a function of precipitation amount (MAP), whereas those in C_4 plants primarily formulates temperature (MAT).

The isotopic fractionation during biosynthesis (ε_{lipid}) from the lipid to bulk leaf tissue varies with plant types. The ε_{lipid} values are -5.2‰, -7.4‰, -7.3‰ and -6.0‰ for trees, shrubs, forbs and C_3 graminoids, respectively, while C_4 graminoids at -9.3‰ are more negative in angiosperms at the global scale (Diefendorf and Freimuth, 2017). Grown under the same environmental condition, conifer trees have smaller ε_{lipid} values than angiosperm trees (-2.5‰ vs. -4.5‰; Diefendorf et al., 2011). In an updated study, Diefendorf et al. (2015) reported a wide range in ε_{lipid} values among conifer families with the smallest values in Pinaceae, intermediate in Cupressaceae and largest in Taxaceae by analyzing a large dataset of conifer species (Diefendorf et al., 2015). The difference in ε_{lipid} values among plant types is probably due to variation in carbon

storage and allocation (Freeman and Pancost, 2014), at least in conifer species (Diefendorf et al., 2015). Factors such as photosynthetic pathway, life form and leaf lifespan are known to be important to control ε_{lipid} values (Diefendorf et al., 2011; Magill et al., 2013). It is complicated to disentangle climate effects from plant type changes on ε_{lipid} values among varied biomes at largely spatial zones. The effect of plant types on ε_{lipid} values is lacking in this study because there were few literatures we compiled that the paired-measurements of lipid $\delta^{13}C_{wax}$ values to bulk leaf tissue $\delta^{13}C$ values were simultaneously conducted, so it is needed to perform the analysis of the effect of plant types on ε_{lipid} values in the future researches.

6. Relationships and inter-calibrations for paleoenvironmental reconstruction

The effects of plan types, three forms of expression (non-wood vs. wood, dicot vs. monocot, C_3 vs. C_4), on leaf wax *n*-alkane biomarkers (*n*-alkane distributions, δ^2H_{wax} and $\delta^{13}C_{wax}$ values) were illustrated in Fig. 11. As above discussion, the *n*-alkane distributions (ACL and CPI) differ significantly between non-woods and woods at each climate zones, instead of those at global scale; the δ^2H_{wax} and $\delta^{13}C_{wax}$ values were significantly different between dicots and monocots and between C_3 and C_4 plants, respectively, which apply consistently with global scale and climate zones. Thus, the plant types do exert significant effects on leaf wax *n*-alkane biomarkers in terrestrial higher plants.

Interpreting leaf wax *n*-alkane biomarkers in sediments as signals of paleohydroclimate, paleovegetation, and paleoaltitude is complicated by the competing effects of climate, geography, and plant types (Fig. 12). Although the overall processes and relative factors are increasingly improved for δ^2H_{wax} (Sachse et al., 2012) and $\delta^{13}C_{wax}$ values (Diefendorf and Freimuth, 2017), the multi-proxy approach provides an effective cross-check of leaf wax biomarkers. This can resolve the ambiguity derived from a single-proxy error, associated with environmental and biological changes in paleoenvironmental reconstruction (Hren et al., 2010; Ernst et al., 2013; Feng et al., 2019; Wang et al., 2021).

The *n*-alkane distribution, such as ACL, CPI and the ratio of $C_{31}/(C_{29} + C_{31})$ *n*-alkanes (Figs. 3, 4), can reveal signals of vegetation change (e.g. Schefuβ et al., 2003; Horikawa et al., 2010; Castañeda et al., 2016; Howard et al., 2018). For example, the $C_{31}/(C_{29}+C_{31})$ ratio and ACL records clearly showed terrestrial landscape variations during the glacial/interglacial cycles over past 800 ka, suggesting a major vegetation transition from grasses to trees associated with the Mid-Brunhes Event in subtropical southern East Africa (Fig. 13a; Castañeda et al., 2016). The $\delta^{13}C_{wax}$ biomarker was widely used in reconstruction of paleovegetation (C_3/C_4 plant ratio; Huang et al., 2001; Wang et al., 2013; Schefuß et al., 2003; Dubois et al., 2014; Castañeda et al., 2016; Fornace et al., 2016), where C_3/C_4 vegetation changes were highly sensitive to hydrology and climate. The combination of *n*-alkane distribution and $\delta^{13}C_{wax}$ biomarkers will be helpful to reconstruct paleoclimate (e.g., hydrology, temperature)

when paleoecology can be constrained through *n*-alkane distributions in some biomes or biome transitions through time. It is possible to exploit differences in *n*-alkane distributions between plant groups to constrain plant wax sources and to provide group-specific $\delta^{13}C$ values, e.g., *n*-C_{29} for C_3 plants and both *n*-C_{33} and *n*-C_{35} for C_4 plants (Garcin et al., 2014). For instance, Schefuß et al. (2003) has reconstructed African C_4 plant abundance based on $\delta^{13}C$ of C_{31} *n*-alkane records at ODP Site 1077 between 1.2 and 0.45 million years ago (Fig. 13b), and they found that African C_4 vegetation variations were controlled by tropical sea surface temperatures in the mid-Pleistocene period.

The *n*-alkane distribution and $\delta^{13}C_{wax}$ values have great potential to disentangle hydroclimatic signals from plant type effects in sedimentary $\delta^{2}H_{wax}$ values (Cranwell, 1984; Meyers, 2003; Luo et al., 2012; Wang et al., 2013; Fornace et al., 2016; Liu et al., 2018). Terrestrial $\delta^{2}H_{wax}$ biomarker can be used as a proxy for reconstructing paleoprecipitation changes, regardless of vapour source effect (Li et al., 2015; Aichner et al., 2022), because $\delta^{2}H_{wax}$ values are strongly correlated with precipitation $\delta^{2}H$ in a number of studies (e.g., Sachse et al., 2006, 2012; Liu and Yang, 2008; Hou et al., 2008; Polissar and Freeman, 2010; Garcin et al., 2012; Liu et al., 2016; Feakins et al., 2016a; Zhang et al., 2017; Liu and An, 2019). For example, a concurrent ~50‰ rise in hydrogen isotope composition of C_{31} *n*-alkane at ODP Site 722 from 10 to 5.5 Ma indicated a progressively drier climate, driving the late Miocene expansion of C_4 plants in the Himalayan foreland and Arabian Peninsula (Fig. 13c; Huang et al., 2007).

Notably, the plant type changes (dicots vs. monocots) exert a significant role in the past δ^2H_{wax} values because of monocots ^2H-depleted by 30-50‰ relative to dicots from local to global scales (Figs. 6, 7). The shift between C_4 grasses (monocots) and C_3 dicots explained more than 40% of δ^2H_{wax} changes for *n*-C_{31} and *n*-C_{33} alkanes during the past 37000 years from Zambezi River catchment on the Central African Plateau (Wang et al., 2013). Afterward, Fornace et al. (2016) suggested that the effect of plant type change (e.g., monocots and dicots) on δ^2H_{wax} values can be calibrated by δ^2H_{wax} - $\delta^{13}C_{wax}$ relationship (Fig. 13d).

In addition, the coupled δ^2H_{wax}-$\delta^{13}C_{wax}$ biomarker is proposed as a paleoelevation proxy in a humid elevation transect (Feakins et al., 2018). The altitudinal effect on δ^2H_{wax} values can be well archived into soils and sediments (Jia et al., 2008; Luo et al., 2011; Nieto-Moreno et al., 2016; Zhang et al., 2017; Liu and An, 2021), which has be used as a proxy for paleoelevation reconstruction in the Tibetan Plateau (Polissar et al., 2009; Zhuang et al., 2014; Bai et al., 2015; Feng et al., 2019), and on the mountains in America (Anderson et al., 2015) and the southern Andes (Nieto-Moreno et al., 2016). Recently, studies show that $\delta^{13}C_{wax}$ values are ^{13}C-enriched with altitude in humid tropical regions in both plants (Wu et al., 2017) and surface soils (Feakins et al., 2018). The dual-isotope approach of coupled δ^2H_{wax}-$\delta^{13}C_{wax}$ biomarkers resolved the ambiguity introduced by the use of δ^2H_{wax} paleoelevation proxy (Feakins et al., 2018). However, my recent investigation showed that the coupled δ^2H_{wax}-$\delta^{13}C_{wax}$ biomarker appears to be not robust in an arid elevation transect on the Chinese Loess Plateau

(Liu, 2021), suggesting that aridity likely affect the reliability of the coupled δ^2H_{wax}-$\delta^{13}C_{wax}$ biomarker as a paleoelevation proxy. It is necessary to identify other proxies to supplement δ^2H_{wax} values under a dual-proxy approach in future research.

7. Potentials and constraints for paleoenvironmental reconstruction

Some advantages of using leaf wax *n*-alkane biomarkers over other terrestrial proxies such as carbonates and stalagmites in paleoenvironmental reconstruction (Rowley and Garzione, 2007; Cheng et al., 2016) have been proved to be possessed: 1) Paleoenvironmental reconstruction can also be determined at sites where no carbonates are present, but where organic material has been preserved; 2) A high-resolution paleoenvironmental record is likely to be achieved because the biosynthesis of leaf wax *n*-alkanes is a relatively short-term process compared with the formation and precipitation of minerals; and 3) The uncertainty from the temperature effect during mineral formation can be largely avoided by the use of leaf wax biomarkers (Peters et al., 2009; Liu and An, 2018). The weaknesses of leaf wax biomarkers for paleoenvironmental proxies are 1) a limited data can be compiled because of time-consuming workload, 2) both plant types and hydroclimate signals are recorded in leaf wax *n*-alkane biomarkers in sediments and 3) the source uncertainty of leaf wax *n*-alkanes in sedimentary records.

Sediments accumulate mixtures of waxes from plants via three dominant modes: waxes attached to leaves (Freimuth et al., 2019), aerosol particulate waxes (Nelson et

al., 2018), and soil-derived waxes by rivers or overland flow (Diefendorf and Freimuth, 2017). Surveys of most lake sediments and surrounding plants suggest that leaf wax input tend to be dominated by direct leaf waxes of local woody plants surrounding the lakes (Cranwell et al., 1987; Sachse et al., 2006, 2012; Seki et al., 2010; Diefendorf et al., 2011; Tipple and Pagani, 2013; Freimuth et al., 2019). Aerosol particulate waxes are an effective pathway for transporting fresh, regional-scale waxes to sediments (Meyers and Hites, 1982; Nelson et al., 2018). River transport of soil-derived waxes is another major pathway that delivers terrestrial waxes to marine and lake sediments (Freimuth et al., 2019). Collectively, the composition of sedimentary waxes contains a mixture of various pathways that vary based on multiple factors such as spatiotemporal variability of vegetation covers in the source region (Gao et al., 2014a), catchment structure depending on lake size, catchment area, connections to rivers and surrounding vegetation cover (Feakins et al., 2018) and the variable influence of atmospheric deposition over different geographic scales (Freimuth et al., 2019).

In particular, even when restricted to *n*-alkanes, they could be derived from sources other than leaves, such as roots (Huang et al., 2011; Liu et al., 2019), especially from wetland plants (He et al., 2020), microbial sources (Li et al., 2018; Chen et al., 2019, 2021), and aerosol deposition (Nelson et al., 2018). Therefore, when there was a significant shift for *n*-alkane sources (e.g., more or less microbial inputs of *n*-alkanes in sedimentary records), leaf wax *n*-alkane isotopic signals may not be best suited for

paleoenvironmental reconstructions, or the interpretation should be carefully approached. For instance, although plant leaf wax was the dominant source of long-chain *n*-alkanes to surface sediments, some aquatic plants could be an important source of long-chain *n*-alkanes to sediments in the lacustrine environment (Aichner et al., 2010; Liu et al., 2015; Andrae et al., 2021). In addition, more ^{13}C enriched and more ^{2}H enriched or depleted values were observed for *n*-alkanes in roots compared with those of leaves in wetland plants (He et al., 2020). Similar significant differences in *n*-alkane $\delta^{2}H$ and $\delta^{13}C$ values of leaves vs. roots were also observed in multiple C_3 grasses and a shrub species (Gamarra and Kahmen, 2015; Liu et al., 2019).

Microbial input (e.g., fungi and bacteria) of long-chain *n*-alkanes have gained increasing attention (Jones, 1969; Li et al., 2018; Chen et al., 2021). Li et al. (2018) performed laboratory incubation and found that the microbial contribution to long-chain *n*-alkanes can reach up to 0.1% per year in aerobic conditions. Therefore, prolonged exposure to aerobic conditions can lead to accumulation of microbially derived long-chain *n*-alkanes while degradation of original *n*-alkanes of leaf wax origin in sediments; hence the impact of microbial contribution to long-chain *n*-alkanes in sediments should be constrained when interpreting sedimentary records of long-chain *n*-alkanes (including the chain length distributions and isotopic ratios). Chen et al. (2019), for the first time, showed that long-chain *n*-alkyl lipids (including *n*-alkanes) can predominantly originate from aquatic microbial sources from sediment samples at three high-latitude (>69 °S latitude) Antarctic lakes, where no vascular

plants are surrounded. Exceptionally high carbon isotopic values (up to –12‰) were obtained for these long-chain *n*-alkyl lipids, which also exclude the possibility of inputs from wind or aerosol transport from adjacent vegetated land masses. A subsequent study further showed that sedimentary long-chain *n*-alkanes in two desolate Antarctic ponds displayed hydrogen isotopic values up to 300‰ higher than those of lake water (Chen et al., 2021). Incorporated with preliminary 16S rRNA gene sequencing data and recent experimental data on microbial hydrogen isotopic fractionation, the authors stated that their data can only be explained by the predominant production of long-chain *n*-alkanes from heterotrophic microbes (Chen et al., 2021).

In this regard, when interpreting sedimentary records, multiple biomarkers are encouraged to analyze simultaneously in addition to *n*-alkanes (He et al., 2018; Liu et al., 2020). For instance, various series of biomarkers other than *n*-alkanes can be identified simultaneously in the aliphatic hydrocarbon fraction when analyzing *n*-alkanes, such as branched alkanes (including highly branched isoprenoids), hopanes and steranes (hopenes and sterenes), botrycoccenes, triterpenes (including des-A-triterpenes) and others (Gao et al., 2007; He et al., 2018; Huang et al., 2013, 2014). Making full use of these hydrocarbon biomarkers accompanied with *n*-alkanes won't introduce additional lab work but can better constrain if there is a significant input of microbial inputs or specific inputs from angiosperm in the studied settings. In addition, statistical analyses and even machine learning approaches could be

introduced to better constrain the sources of *n*-alkanes in sediments and expand their applicability for paleoreconstructions (Peaple et al., 2021).

Considering the rapidly increasing importance of leaf wax *n*-alkanes in paleoclimate and paleoenvironmental studies, considerable efforts should be made to investigate leaf wax *n*-alkane biomarkers in modern plants at high-resolution spatial and temporal scales because the modern plant analysis builds a foundation for biomarker-based reconstructions in the future (e.g., Chikaraishi and Naraoka, 2003; Liu et al., 2006; Hou et al., 2007; Sachse et al., 2012; Garcin et al., 2014; Feakins et al., 2016a; Zhang et al., 2017; Diefendorf and Freimuth, 2017; Liu and An, 2019, 2020; He et al., 2020) and examine the controls and relationships between leaf wax biomarkers and hydroclimate factors apart from the effect of plant types on leaf wax biomarkers. The dual-proxy or multi-proxy coupling provides an effective tool to reduce the ambiguity and uncertainties derived from a single proxy and disentangle hydroclimate signals from plant type effects in sedimentary leaf wax biomarkers, but it needs to be firstly tested in *in-situ* modern plants. In addition, understanding and constraining the contribution of microbially-derived mid- and long-chain *n*-alkanes in the studied setting and mechanistic understanding of how diagenesis affects the *n*-alkane isotopic signal are also critical to better constrain the applicability of *n*-alkanes in paleoreconstructions.

8. Conclusion

The plant type effects, three forms of expression (non-wood vs. wood, dicot vs. monocot, C_3 vs. C_4), on leaf wax *n*-alkane biomarkers (*n*-alkane distributions, δ^2H_{wax} and $\delta^{13}C_{wax}$ values) were well demonstrated. It is crucially critical to disentangle hydroclimate signals from plant type effects in sedimentary leaf wax biomarkers when leaf wax *n*-alkane biomarkers are utilized to reconstruct paleoenvironments. Our results were showed as follows:

1) The *n*-alkane distributions, characterized by ACL and CPI, differ more significantly at climate zone scale than global scale. The *n*-alkane distributions are much helpful to interpret plant type information (non-wood vs. wood) at local and regional scale, instead of global scale.
2) The δ^2H_{wax} biomarker varies significantly between dicots and monocots, with dicots ^2H-enriched by ~30‰ relative to monocots. The global mean ε_{app} values are -107 ± 28.5‰ and -142 ± 28.5‰ for dicots and monocots, respectively. Such differences in ε_{app} values between dicots and monocots persist steadily across climate zones.
3) The $\delta^{13}C_{wax}$ biomarker differs significantly between C_3 and C_4 plants at both climate zones and global scales. The global mean $\delta^{13}C_{wax}$ values were -35.0±3.2 and -21.9±2.4 for C_3 and C_4 plants, respectively.
4) The multi-proxy approach provides an effective cross-check among three forms of leaf wax *n*-alkane biomarkers. The combination of *leaf wax n-alkane* biomarkers will be helpful to reconstruct paleohydroclimates when paleoecology can be constrained by using *n*-alkane distributions.

5) The transport pathways and microbial input to sediments should be also considered when interpreting sedimentary records of long-chain *n*-alkanes.

Acknowledgments

We would like to thank C. Zhao for comments on earlier versions of the manuscript. Thanks to Y. Cheng for compiling data from the literature. This review was supported by the Chinese Academy of Sciences (XDB40000000; ZDBS-LY-DQC033; 132B61KYSB20170005; XAB2019B02) and the National Natural Science Foundation of China (42073017; 42030512).

Author contribution

J.L. conceived the idea of research. J.L. and C. J. performed the data analysis. J.L., J.Z. and D.H. wrote the manuscript. All authors contributed to discuss the results.

Competing interests

The authors declare that they have no known competing financial interests or personal relationships that could have appeared to influence the work reported in this paper.

Appendix

1. The ACL and CPI of long-chain *n*-alkanes using the following equations (Liu et al., 2018):

$$ACL = \frac{27\times C_{27}+29\times C_{29}+31\times C_{31}+33\times C_{33}+35\times C_{35}+37\times C_{37}}{C_{27}+C_{29}+C_{31}+C_{33}+C_{35}+C_{37}}$$

and

$$CPI = \frac{(C_{27}+C_{29}+C_{31}+C_{33}+C_{35})+(C_{29}+C_{31}+C_{33}+C_{35}+C_{37})}{2\times(C_{28}+C_{30}+C_{32}+C_{34}+C_{36})}$$

2. The apparent hydrogen isotopic fractionation factor (ε_{app}) between leaf wax and precipitation is determined as the following (Liu et al., 2016):

$$\varepsilon_{app} = (\frac{\delta^2H_{wax}+1000}{\delta^2H_p+1000} - 1)\times 1000$$

3. The carbon isotope fractionation during biosynthesis is commonly quantified by

$$\varepsilon_{lipid} = (\frac{\delta^{13}C_{lipid}+1000}{\delta^{13}C_{leaf}+1000} - 1)\times 1000$$

where the carbon isotopic composition of the lipid of interest is compared with bulk leaf tissue (Chikaraishi et al., 2004).

References

Aichner, B., Herzschuh, U., Wilkes, H., 2010. Influence of aquatic macrophytes on the stable carbon isotopic signatures of sedimentary organic matter in lakes on the Tibetan Plateau. *Organic Geochemistry*, 41, pp.706-718.

Aichner, B., Wünnemann, B., Callegaro, A., van der Meer, M.T.J., Yan, D., Zhang, Y., Barbante, C., Sachse, D., 2022. Asynchronous responses of aquatic ecosystems to hydroclimatic forcing on the Tibetan Plateau. *Communications Earth & Environment*, 3, 3. https://doi.org/10.1038/s43247-021-00325-1.

Ali, H.A.M., Mayes, R.W., Hector, B.L., Orskov, E.R., 2005a. Assessment of *n*-alkanes, long-chain fatty alcohols and long-chain fatty acids as diet composition

markers: The concentrations of these compounds in rangeland species from Sudan. *Animal Feed Science and Technology*, 121, pp. 257-271.

Ali, H.A.M., Mayes, R.W., Hector, B.L., Verma, A.K., Ørskov, E.R., 2005b. The possible use of *n*-alkanes, long-chain fatty alcohols and long-chain fatty acids as markers in studies of the botanical composition of the diet of free-ranging herbivores. *Journal of Agricultural Science*, 143, pp.85-95.

Anderson, V., Saylor, J., Shanahan, T. and Horton, B., 2015. Paleoelevation records from lipid biomarkers: Application to the tropical Andes. *Geological Society of America Bulletin*, 127(11-12), pp.1604-1616.

Andrae, J.W., McInerney, F.A., Sniderman, J.M.K., 2020. Carbon isotope systematics of leaf wax n-alkanes in a temperate lacustrine deposition environment. *Organic Geochemistry*, 150, 104121.

Ankit, Y., Mishra, P., Kumar, P., Jha, D., Kumar, V., Ambili, V. and Anoop, A., 2017. Molecular distribution and carbon isotope of *n*-alkanes from Ashtamudi Estuary, South India: Assessment of organic matter sources and paleoclimatic implications. *Marine Chemistry*, 196, pp.62-70.

Ardenghi, N., Mulch, A., Pross, J. and Maria Niedermeyer, E., 2017. Leaf wax *n*-alkane extraction: An optimised procedure. *Organic Geochemistry*, 113, pp.283-292.

Avato, P., Bianchi, G., Mariani, G., 1984. Epicuticular waxes of sorghum and some compositional changes with plant age. *Phyrochemirrry,* 23, pp.2843-2846.Badewien,

T., Vogts, A. and Rullkötter, J., 2015. *n*-Alkane distribution and carbon stable isotope composition in leaf waxes of C_3 and C_4 plants from Angola. *Organic Geochemistry*, 89-90, pp.71-79.

Bai, Y., Fang, X., Gleixner, G., Mügler, I., 2011. Effect of precipitation regime on δD values of soil *n*-alkanes from elevation gradients - Implications for the study of paleo-elevation. *Organic Geochemistry*, 42, pp.838-845.

Bai, Y., Tian, Q., Fang, X., Wu, F., 2014. The "inverse altitude effect" of leaf wax-derived *n*-alkane δD on the northeastern Tibetan Plateau. *Organic Geochemistry*, 73, pp.90-100.

Bai, Y., Fang, X., Jia, G., Sun, J., Wen, K. and Ye, Y., 2015. Different altitude effect of leaf wax *n*-alkane δD values in surface soils along two vapor transport pathways, southeastern Tibetan Plateau. *Geochimica et Cosmochimica Acta*, 170, pp.94-107.

Bai, Y., Azamdzhon, M., Wang, S., Fang, X., Guo, H., Zhou, P., Chen, C., Liu, X., Jia, S., Wang, Q., 2019. An evaluation of biological and climatic effects on plant *n*-alkane distributions and δ^2H_{alk} in a field experiment conducted in central Tibet. *Organic Geochemistry*, 135, pp.53-63.

Bai, Y., Tian, Q., Fang, X., Chen, C. and Liu, X., 2020. Responses of sedimentary δ^2H_{alk} values to environmental changes as revealed by different plant responses to altitude and altitude-related temperatures. *Science of The Total Environment*, 733, p.138087.

Balascio, N.L., D'Andrea, W.J., Anderson, R.S., Wickler, S., 2018. Influence of vegetation type on *n*-alkane composition and hydrogne iostope values from a high latitude ombrotropica bog. *Organic Geochemistry*, 121, pp.48-57.

Barbour, M., 2007. Stable oxygen isotope composition of plant tissue: a review. *Functional Plant Biology*, 34(2), p.83.

Berke, M.A., Sierra, A.C., Bush, R., Cheah, D., O'Connor, K., 2019. Controls on leaf wax fractionation and δ^2H values in tundra vascular plants from western Greenland. *Geochimica et Cosmochimica Acta*, 244, pp.565-585.

Bezabih, M., Pellikaan, W.F., Tolera, A., Hendriks, W.H., 2011. Evaluation of *n*-alkanes and their carbon isotope enrichments as diet composition markers. *Animal*, 5, pp.57-66.

Bi, X., Sheng, G., Liu, X., Li, C. and Fu, J., 2005. Molecular and carbon and hydrogen isotopic composition of n-alkanes in plant leaf waxes. *Organic Geochemistry*, 36(10), pp.1405-1417.

Bojović, S., Šarac, Z., Nikolić, B., Tešević, V., Todosijević, M., Veljić, M., Marinf, P.D., 2012. Composition of *n*-Alkanes in Natural Populations of Pinus nigra from Serbia-Chemotaxonomic Implications. *CHEMISTRY & BIODIVERSITY*, 9, pp.2761-2774.

Boom, A., Carr, A., Chase, B., Grimes, H. and Meadows, M., 2014. Leaf wax *n*-alkanes and $\delta^{13}C$ values of CAM plants from arid southwest Africa. *Organic Geochemistry*, 67, pp.99-102.

Brittingham, A., Hren, M.T., Hartman, G., 2017. Microbial alteration of the hydrogen and carbon isotopic composition of *n*-alkanes in sediments. *Organic Geochemistry*, 107, 1-8.

Bugalho, M.N., Dove, H., Kelman, W., Wood, J.T., Mayes, R.W., 2004. Plant wax alkanes and alcohols as herbivore diet composition markers. *JOURNAL OF RANGE MANAGEMENT*, 57, pp.258-268.

Burnham, R., 1989. Relationships between standing vegetation and leaf litter in a paratropical forest: Implications for paleobotany. *Review of Palaeobotany and Palynology*, 58(1), pp.5-32.

Burnham, R., Wing, S. and Parker, G., 1992. The reflection of deciduous forest communities in leaf litter: implications for autochthonous litter assemblages from the fossil record. *Paleobiology*, 18(1), pp.30-49.

Bush, M., 2002. On the interpretation of fossil Poaceae pollen in the lowland humid neotropics. *Palaeogeography, Palaeoclimatology, Palaeoecology*, 177(1-2), pp.5-17.

Bush, R. and McInerney, F., 2013. Leaf wax *n*-alkane distributions in and across modern plants: Implications for paleoecology and chemotaxonomy. *Geochimica et Cosmochimica Acta*, 117, pp.161-179.

Bush, R., McInerney, F., 2015. Influence of temperature and C_4 abundance on *n*-alkane chain length distributions across the central USA. *Organic Geochemistry*, 79, pp.65-73.

Carr, A., Boom, A., Grimes, H., Chase, B., Meadows, M. and Harris, A., 2014. Leaf wax n-alkane distributions in arid zone South African flora: Environmental controls, chemotaxonomy and palaeoecological implications. *Organic Geochemistry*, 67, pp.72-84.

Castañeda, I., Caley, T., Dupont, L., Kim, J., Malaizé, B. and Schouten, S., 2016. Middle to Late Pleistocene vegetation and climate change in subtropical southern East Africa. *Earth and Planetary Science Letters*, 450, pp.306-316.

Castillo, J.B.D., Brooks, C.J.W., Cambie, R.C., Eglinton, G., Hamilton, R.J., Pellitt, P., 1967. The taxonomic distribution of some hydrocarbons in gymnosperms. *Phytochemistry*, 6, pp.391-398.

Ceccopieri, M., Scofield, A.L., Almeida, L., Araújo, M.P., Hamacher, C., Farias, C.O., Soares, M.L.G., Carreira, R.S., Wagener A.L. R., 2021, Carbon isotopic composition of leaf wax *n*-alkanes in mangrove plants along a latitudinal gradient in Brazil. *Organic Geochemistry*, 161. pp.104299.

Cerda-Peña, C., Contreras, S., Rau, J.R., 2020. Molecular *n*-alkyl leaf waxes of three dominant plants from the temperate forest in South America. *Organic Geochemistry*, 149, pp.104105.

Cernusak, L., Ubierna, N., Winter, K., Holtum, J., Marshall, J. and Farquhar, G., 2013. Environmental and physiological determinants of carbon isotope discrimination in terrestrial plants. *New Phytologist*, 200(4), pp.950-965.

Chen, W., Lefroy, R.D.B., Blair, G.J., Scott, J.M., 1998. Field variations in alkane signatures among plant species in 'degraded' and perennial pastures on the Northern Tablelands of New South Wales. *Australian Journal of Agricultural Research*, 49, pp.263-268.

Chen, X., Liu, X., Wei, Y. and Huang, Y., 2019. Production of long-chain *n*-alkyl lipids by heterotrophic microbes: New evidence from Antarctic lakes. *Organic Geochemistry*, 138, p.103909.

Chen, X., Liu, X., Jia, H., Jin, J., Kong, W. and Huang, Y., 2021. Inverse hydrogen isotope fractionation indicates heterotrophic microbial production of long-chain n -alkyl lipids in desolate Antarctic ponds. *Geobiology*, 19(4), pp.394-404.

Chikaraishi, Y. and Naraoka, H., 2003. Compound-specific δD–δ^{13}C analyses of *n*-alkanes extracted from terrestrial and aquatic plants. *Phytochemistry*, 63(3), pp.361-371.

Chikaraishi, Y., Naraoka, H., Poulson, S.R., 2004. Carbon and hydrogen isotopic fractionation during lipid biosynthesis in a higher plant (Cryptomeria japonica). *Phytochemistry,* 65, pp.323-330.Chikaraishi, Y., Naraoka, H., 2006. Carbon and hydrogen isotope variation of plant biomarkers in a plant-soil system. *Chemical Geology,* 231, pp.190-202.

Cifuentes, G., Contreras, S., Cerda-Peña, C., 2020. Evaluation of the Foliar Damage That Threatens a Millennial-Age Tree, Araucaria araucana (Molina) K.Koch, Using Leaf Waxes. *Forests,* 11, p.59.

Collatz, G., Berry, J. and Clark, J., 1998. Effects of climate and atmospheric CO_2 partial pressure on the global distribution of C_4 grasses: present, past, and future. *Oecologia*, 114(4), pp.441-454.

Collister, J., Rieley, G., Stern, B., Eglinton, G. and Fry, B., 1994. Compound-specific $\delta^{13}C$ analyses of leaf lipids from plants with differing carbon dioxide metabolisms. *Organic Geochemistry*, 21(6-7), pp.619-627.

Conte, M.H., Weber, J.C., Carlson, P.J., Flanagan, L.B., 2003. Molecular and carbon isotopic composition of leaf wax in vegetation and aerosols in a northern prairie ecosystem. *Oecologia,* 135, pp.67-77.

Collins, J.A., Schefuß, E., Mulitza, S., Prange, M., Werner, M., Tharammal, T., Paul, A., Wefer, G., 2013. Estimating the hydrogen isotopic composition of past precipitation using leaf-waxes from western Africa. Quaternary Science Reviews, 65, pp.88 – 101.

Cormier, M.-A., Werner, R.A., Sauer, P.E., Gröcke, D.R., Leuenberger, M.C., Wieloch, T., Schleucher, J., Kahmen, A., 2018. ^{2}H-fractionations during the biosynthesis of carbohydrates and lipids imprint a metabolic signal on the δ2H values of plant organic compounds. *New Phytologist*, 218, pp.479 – 491.

Cranwell, P., 1973. Chain-length distribution of n-alkanes from lake sediments in relation to post-glacial environmental change. *Freshwater Biology*, 3(3), pp.259-265.

Cranwell, P., 1984. Alkyl esters, mid chain ketones and fatty acids in late glacial and postglacial lacustrine sediments. *Organic Geochemistry*, 6, pp.115-124.

Cranwell, P., Eglinton, G. and Robinson, N., 1987. Lipids of aquatic organisms as potential contributors to lacustrine sediments—II. *Organic Geochemistry*, 11(6), pp.513-527.

Diefendorf, A., Mueller, K., Wing, S., Koch, P. and Freeman, K., 2010. Global patterns in leaf 13C discrimination and implications for studies of past and future climate. *Proceedings of the National Academy of Sciences*, 107(13), pp.5738-5743.

Diefendorf, A., Freeman, K., Wing, S. and Graham, H., 2011. Production of *n*-alkyl lipids in living plants and implications for the geologic past. *Geochimica et Cosmochimica Acta*, 75(23), pp.7472-7485.

Diefendorf, A., Leslie, A. and Wing, S., 2015. Leaf wax composition and carbon isotopes vary among major conifer groups. *Geochimica et Cosmochimica Acta*, 170, pp.145-156.

Diefendorf, A. and Freimuth, E., 2017. Extracting the most from terrestrial plant-derived n-alkyl lipids and their carbon isotopes from the sedimentary record: A review. *Organic Geochemistry*, 103, pp.1-21.

Daniels, W., Russell, J., Giblin, A., Welker, J., Klein, E. and Huang, Y., 2017. Hydrogen isotope fractionation in leaf waxes in the Alaskan Arctic tundra. *Geochimica et Cosmochimica Acta*, 213, pp.216-236.

Dion-Kirschner, H., McFarlin, J.M., Masterson, A.L., Axford, Y., Osburn, M.R., 2020. Modern constraints on the sources and climate signals recorded by sedimentary plant waxes in west Greenland. *Geochimica et Cosmochimica Acta*, 286, pp.336-354.

Dodoš, T., Rajčević, N., Tešević, V., Matevski, V., Janaćković, P., Marin, P.D., 2015. Composition of Leaf *n*-Alkanes in Three Satureja montana L. Subspecies from the Balkan Peninsula: Ecological and Taxonomic Aspects. *CHEMISTRY & BIODIVERSITY*, 12, pp.157-169.

Douglas, P., Pagani, M., Brenner, M., Hodell, D. and Curtis, J., 2012. Aridity and vegetation composition are important determinants of leaf-wax δD values in southeastern Mexico and Central America. *Geochimica et Cosmochimica Acta*, 97, pp.24-45.

Dove, H., 1992. Using the *n*-alkanes of plant cuticular wax to estimate the species composition of herbage mixtures. *Aust. J. Agric. Res.*, 43, pp.1711-1724.

Dove, H., Mayes, R.W., 2005. Using *n*-alkanes and other plant wax components to estimate intake, digestibility and diet composition of grazing/browsing sheep and goats. *Small Ruminant Research*, 59, pp.123-139.

Duan, Y., Zheng, C., Wu, B., 2010. Hydrogen isotopic characteristics and their genetic relationships for individual *n*-alkanes in plants and sediments from Zoige marsh sedimentary environment. *Science China Earth Science*, 40, pp.745-750 (in Chinese).

Duan, Y. and He, J., 2011a. Distribution and isotopic composition of *n*-alkanes from grass, reed and tree leaves along a latitudinal gradient in China. *Geochemical Journal*, 45(3), pp.199-207.

Duan, Y., Jia, X., He, J., Zhang, X., Xu, L., Wu, B., 2011b. *n*-alakens and their hydrogen isotopic compositions of sediments in Chaka Salt lake and terrestrial plants in adjacent area. *Acta Geologica Sinica,* 85, pp.2084-2092 (in Chinese).

Duan, Y., Wu Y., Cao X., Zhao Y., Ma L., 2014. Hydrogen isotope ratios of individual *n*-alkanes in plants from Gannan Gahai Lake (China) and surrounding area.*Organic Geochemistry,* 77, pp.96-105.

Duan, Z.H., Quan, X.L., Qiao, Y.M., Pei, H.K., 2016. Characterization of plant *n*-alkanes in alpine meadow. Acta Prataculturae Sinica, 25, pp.136-147.

Duan, Y., Wu, Y., Wu, B., Sun, T., 2018. Hydrogen isotope compositions and influencing factors of *n*-alaknes in organisms from the Qinghai Lake areas. *Acta Geologica Sinica,* 92, pp.1541-1550 (in Chinese).

Dubois, N., Oppo, D., Galy, V., Mohtadi, M., van der Kaars, S., Tierney, J., Rosenthal, Y., Eglinton, T., Lückge, A. and Linsley, B., 2014. Indonesian vegetation response to changes in rainfall seasonality over the past 25,000 years. *Nature Geoscience,* 7(7), pp.513-517.

Edwards, G., Nakamoto, H., Burnell, J. and Hatch, M., 1985. Pi dikinase and NADP-malate dehydrogenase in C4 photosynthesis: properties and mechanism of light/dark regulation. *Annual Review of Plant Physiology,* 36(1), pp.255-286.

Eglinton, G., Hamilton, R.J., Martin-Smith, M., 1962. The alkane constituents of some New Zealand plants and their possible taxonomic implications. *Phytochemistry,* 1, pp.137-145.

Eglinton, G. and Hamilton, R., 1963. The distribution of alkanes. In: Swain, T. (Ed.), Chemical Plant Taxonomy. *Academic Press*, pp. 187–217.

Eglinton, G. and Hamilton, R., 1967. Leaf epicuticular waxes. *Science*, 156(3780), pp.1322-1335.

Eley, Y., Dawson, L., Black, S., Andrews, J., Pedentchouk, N., 2014. Understanding $^{2}H/^{1}H$ systematics of leaf wax *n*-alkanes in coastal plants at Stiffkey saltmarsh, Norfolk, UK. *Geochimica et Cosmochimica Acta*, 128, pp.13-28.

Eley, Y., Dawson, L., Pedentchouk, N., 2016. Investigating the carbon isotope composition and leaf wax *n*-alkane concentration of C_3 and C_4 plants in Stiffkey saltmarsh, Norfolk, UK. *Organic Geochemistry*, 96, pp.28-42.

Eley, Y. and Hren, M., 2018. Reconstructing vapor pressure deficit from leaf wax lipid molecular distributions. *Scientific Reports*, 8(1).

Ellis, B. and Johnson, K., 2013. Comparison of leaf samples from mapped tropical and temperate forests: implications for interpretations of the diversity of fossil assemblages. *Palaios*, 28(3), 163–177.

Evans, J., Sharkey, T., Berry, J. and Farquhar, G., 1986. Carbon Isotope Discrimination measured concurrently with gas exchange to investigate CO_2 diffusion in leaves of higher plants. *Functional Plant Biology*, 13(2), p.281.

Farquhar, G., O'Leary, M. and Berry, J., 1982. On the relationship between carbon isotope discrimination and the intercellular carbon dioxide concentration in leaves. *Functional Plant Biology*, 9(2), p.121.

Farquhar, G., Hubick, K., Condon, A. and Richards, R., 1988. Carbon isotope fractionation and plant water-use efficiency. In: Rundel, P., Ehleringer, R. and Nagy, K. (Eds.), *Stable Isotopes in Ecological Research*, pp. 21–40.

Farquhar, G., Ehleringer, J. and Hubick, K., 1989. Carbon isotope discrimination and photosynthesis. *Annual Review of Plant Physiology and Plant Molecular Biology*, 40(1), pp.503-537.

Farquhar, G. and Gan, K., 2003. On the progressive enrichment of the oxygen isotopic composition of water along a leaf. *Plant, Cell & Environment*, 26(9), pp.1579-1597.

Feakins, S. and Sessions, A., 2010a. Controls on the D/H ratios of plant leaf waxes in an arid ecosystem. *Geochimica et Cosmochimica Acta*, 74(7), pp.2128-2141.

Feakins, S., and Sessions, A., 2010b, Crassulacean acid metabolism influences D/H ratio of leaf wax in succulent plants. *Organic Geochemistry*, 41, pp.1269-1276.

Feakins, S., Warny, S. and Lee, J., 2012. Hydrologic cycling over Antarctica during the middle Miocene warming. *Nature Geoscience*, 5(8), pp.557-560.

Feakins, S., Bentley, L., Salinas, N., Shenkin, A., Blonder, B., Goldsmith, G., Ponton, C., Arvin, L., Wu, M., Peters, T., West, A., Martin, R., Enquist, B., Asner, G. and

Malhi, Y., 2016a. Plant leaf wax biomarkers capture gradients in hydrogen isotopes of precipitation from the Andes and Amazon. *Geochimica et Cosmochimica Acta*, 182, pp.155-172.

Feakins, S., Peters, T., Wu, M.S., Shenkin, A., Salinas, N., Girardin, C.A.J., Bentley, L.P., Blonder, B., Enquist, B.J., Martin, R.E., Asner, G.P., Malhi, Y., 2016b. Production of leaf wax *n*-alkanes across a tropical forest elevation transect. *Organic Geochemistry*, 100, pp.89–100.

Feakins, S., Wu, M., Ponton, C., Galy, V. and West, A., 2018. Dual isotope evidence for sedimentary integration of plant wax biomarkers across an Andes-Amazon elevation transect. *Geochimica et Cosmochimica Acta*, 242, pp.64-81.

Feng, X., D'Andrea, W., Zhao, C., Xin, S., Zhang, C. and Liu, W., 2019. Evaluation of leaf wax δD and soil brGDGTs as tools for paleoaltimetry on the southeastern Tibetan Plateau. *Chemical Geology*, 523, pp.95-106.

Ficken, K.J., Barber, K.E., Eglinton, G., 1998. Lipid biomarker, $\delta^{13}C$ and plant macrofossil stratigraphy of a Scottish montane peat bog over the last two millennia. *Organic Geochemistry*, 28, pp.217-237.

Ficken, K.J., Li, B., Swain, D.L., Eglinton, G., 2000. An *n*-alkane proxy for the sedimentary input of submerged/floating freshwater aquatic macrophytes. *Organic Geochemistry*, 31, pp.745 – 749.

Fornace, K., Whitney, B., Galy, V., Hughen, K. and Mayle, F., 2016. Late Quaternary environmental change in the interior South American tropics: new insight from leaf wax stable isotopes. *Earth and Planetary Science Letters*, 438, pp.75-85.

Freeman, K. and Pancost, R., 2014. Biomarkers for terrestrial plants and climate. In: Turekian, H. and Holland, K. (Eds.), *Treatise on Geochemistry (Second Edition)*. Elsevier, pp. 395-416.

Freimuth, E. J., Diefendorf, A. F., Lowell, T. V., 2017. Hydrogen isotopes of *n*-alkanes and *n*-alkanoic acids as tracers of precipitation in a temperate forest and implications for paleorecords. *Geochimica et Cosmochimica Acta*, 206, pp.166-183.

Freimuth, E., Diefendorf, A., Lowell, T. and Wiles, G., 2019. Sedimentary *n*-alkanes and *n*-alkanoic acids in a temperate bog are biased toward woody plants. *Organic Geochemistry*, 128, pp.94-107.

Gamarra, B. and Kahmen, A., 2015. Concentrations and δ2H values of cuticular *n*-alkanes vary significantly among plant organs, species and habitats in grasses from an alpine and a temperate European grassland. *Oecologia*, 178(4), pp.981-998.

Gao, M., Simoneit, B., Gantar, M. and Jaffé, R., 2007. Occurrence and distribution of novel botryococcene hydrocarbons in freshwater wetlands of the Florida Everglades. *Chemosphere*, 70(2), pp.224-236.

Gao, L., Zheng, M., Fraser, M. and Huang, Y., 2014a. Comparable hydrogen isotopic fractionation of plant leaf waxn-alkanoic acids in arid and humid subtropical ecosystems. *Geochemistry, Geophysics, Geosystems*, 15(2), pp.361-373.

Gao, L., Edwards, E. J., Zeng, Y., Huang, Y., 2014b. Major evolutionary trends in hydrogen isotope fractionation of vascular plant leaf waxes. *PlOS ONE,* 9, p.112610.

Garcin, Y., Schwab, V., Gleixner, G., Kahmen, A., Todou, G., Séné, O., Onana, J., Achoundong, G. and Sachse, D., 2012. Hydrogen isotope ratios of lacustrine sedimentary *n*-alkanes as proxies of tropical African hydrology: Insights from a calibration transect across Cameroon. *Geochimica et Cosmochimica Acta*, 79, pp.106-126.

Garcin, Y., Schefuß, E., Schwab, V., Garreta, V., Gleixner, G., Vincens, A., Todou, G., Séné, O., Onana, J., Achoundong, G. and Sachse, D., 2014. Reconstructing C_3 and C_4 vegetation cover using *n*-alkane carbon isotope ratios in recent lake sediments from Cameroon, Western Central Africa. *Geochimica et Cosmochimica Acta*, 142, pp.482-500.

Griepentrog, M., De Wispelaere, L., Bauters, M., Bodé, S., Hemp, A., Verschuren, D., Boeckx, P., 2019. Influence of plant growth form,habitat and season on leafwax *n*-alkane hydrogen isotopic signatures in equatorial East Africa. *Geochimica et Cosmochimica Acta,* 263, pp.122-139.

Gülz, P., Müller, E., Prasad, R.B.N., Organ-specific composition of epicuticular waxes of beech (Fagus sylvatica L.) leaves and seeds. *Z. Naturforsch*, 44, pp.731-734.

Guo, N., Gao, J., He, Y., Zhang, Z., Guo, Y., 2014. Variations in leaf epicuticular *n*-alkanes in some Broussonetia, Ficus and Humulus species. *Biochemical Systematics and Ecology*, 54, pp.150-156.

Guo, Y., He, Y., Guo, N., Gao, J., Ni, Y., 2015. Variations of the Composition of the Leaf Cuticular Wax among Chinese Populations of Plantago major. *CHEMISTRY & BIODIVERSITY,* 12, pp.627-636.

Guo, N., Gao, J., He, Y., Guo, Y., 2016. Compositae Plants Differed in Leaf Cuticular Waxes between High and Low Altitudes. *Chem. Biodiversity,* 13, pp.710-718

Hall, D.M., Matus, A.I., Lamberton, J.A., Barber, H.N., 1966. Infra-specific variation in wax on leaf surfaces. *Aust. J. Biol. Sci.,* 18, pp.323-332.

He, D., Anderson, W. and Jaffé, R., 2016. Compound specific δD and $\delta^{13}C$ analyses as a tool for the assessment of hydrological change in a subtropical wetland. *Aquatic Sciences*, 78(4), pp.809-822.

He, D., Zhang, K., Cui, X., Tang, J. and Sun, Y., 2018. Spatiotemporal variability of hydrocarbons in surface sediments from an intensively human-impacted Xiaoqing River-Laizhou Bay system in the eastern China: Occurrence, compositional profile and source apportionment. *Science of The Total Environment*, 645, pp.1172-1182.

He, D., Nemiah Ladd, S., Saunders, C., Mead, R. and Jaffé, R., 2020. Distribution of *n*-alkanes and their $\delta^{2}H$ and $\delta^{13}C$ values in typical plants along a terrestrial-coastal-oceanic gradient. *Geochimica et Cosmochimica Acta*, 281, pp.31-52.

Helliker, B. and Ehleringer, J., 2000. Establishing a grassland signature in veins: ^{18}O in the leaf water of C_3 and C_4 grasses. *Proceedings of the National Academy of Sciences*, 97(14), pp.7894-7898.

Helliker, B. and Ehleringer, J., 2002. Differential ^{18}O enrichment of leaf cellulose in C_3 versus C_4 grasses. *Functional Plant Biology*, 29(4), p.435.

Herbin, G.A., Robins, P.A., 1968a. Studies on plant cuticular waxes—II: Alkanes from members of the genusAgave (Agavaceae), the generaKalanchoe, Echeveria, Crassula andSedum (Crassulaceae) and the genusEucalyptus (Myrtaceae) with an examination of Hutchinson's sub-division of the Angiosperms into Herbaceae and Lignosae. *Phytochemistry,* 7, pp.257-268.

Herbin, G.A., Robins, P.A., 1968b. Studies on plant cuticular waxes—III. The leaf wax alkanes and ω-hydroxy acids of some members of the Cupressaceae and Pinaceae. *Phytochemlstry,* 7, pp.1325-1337.

Herbin, G.A., Robins, P.A., 1969. Patterns of variation and development in leaf wax alkanes. *Phytochemistry,* 8, pp.1985-1998.

Ho, S., Wang, C., Wang, M., Li, Z., 2015. Effect of petroleum on carbon and hydrogen isotopic composition of long-chain *n*-alkanes in plants from the Yellow River Delta, China. *Environment Earth Science,* 74, pp.1603-1610.

Hockun, K., Mollenhauer, G., Ho, S.L., Hefter, J., Ohlendorf, C., Zolitschka, B., Mayr, C., Lücke, A., Schefuß, E., 2016. Using distributions and stable isotopes of *n*-alkanes to disentangle organic matter contributions to sediments of Laguna Potrok Aike, Argentina. *Organic Geochemistry,* 102, pp.110-119.

Hoffmann, B., Kahmen, A., Cernusak, L., Arndt, S. and Sachse, D., 2013. Abundance and distribution of leaf wax *n*-alkanes in leaves of Acacia and Eucalyptus trees along

a strong humidity gradient in northern Australia. *Organic Geochemistry*, 62, pp.62-67.

Horn, D.H.S., Krakz, Z.H., Lambert, J.A., 1964. The composition of Eucalyptus and some other leaf waxes. *Aust. J. Chem.*, 17, pp.464-476.

Hou, J., D'Andrea, W., MacDonald, D. and Huang, Y., 2007. Hydrogen isotopic variability in leaf waxes among terrestrial and aquatic plants around Blood Pond, Massachusetts (USA). *Organic Geochemistry*, 38(6), pp.977-984.

Hou, J., D'Andrea, W. and Huang, Y., 2008. Can sedimentary leaf waxes record D/H ratios of continental precipitation? Field, model, and experimental assessments. *Geochimica et Cosmochimica Acta*, 72(14), pp.3503-3517.

Hou, J., Tian, Q. and Wang, M., 2018. Variable apparent hydrogen isotopic fractionation between sedimentary *n*-alkanes and precipitation on the Tibetan Plateau. *Organic Geochemistry*, 122, pp.78-86.

Howard, S., McInerney F., Caddy-Retalic, S., Hall, P. and Andrae, J., 2018. Modelling leaf wax *n*-alkane inputs to soils along a latitudinal transect across Australia. *Organic Geochemistry*, 121, pp.126-137.

Huang, X., Wang, C., Zhang, J., Wiesenberg, G., Zhang, Z. and Xie, S., 2011. Comparison of free lipid compositions between roots and leaves of plants in the Dajiuhu Peatland, central China. *Geochemical Journal*, 45(5), pp.365-373.

Huang, X., Xue, J., Wang, X., Meyers, P., Huang, J. and Xie, S., 2013. Paleoclimate influence on early diagenesis of plant triterpenes in the Dajiuhu peatland, central China. *Geochimica et Cosmochimica Acta*, 123, pp.106-119.

Huang, X., Meyers, P., Xue, J., Wang, X. and Zheng, L., 2014. Cryptic abundance of long-chain iso and anteiso alkanes in the Dajiuhu peat deposit, central China. *Organic Geochemistry*, 66, pp.137-139.

Huang, Y., Bol, R., Harkness, D.D., Ineson, P., Eglinton, G., 1996. Post-glacial variations in distributions, ^{13}C and ^{14}C contents of aliphatic hydrocarbons and bulk organic matter in three types of British acid upland soils. Organic Geochemistry, 24(3), pp. 273-287.

Huang, Y., Dupont, L., Sarnthein, M., Hayes, J. and Eglinton, G., 2000. Mapping of C_4 plant input from North West Africa into North East Atlantic sediments. *Geochimica et Cosmochimica Acta*, 64(20), pp.3505-3513.

Huang, Y., Street-Perrott, F.A., Metcalfe, S.E., Brenner, M., Moreland, M., Freeman, K.H., 2001. Climate change as the dominant control on glacial-interglacial variations in C_3 and C_4 Plant Abundance. *Science*, 293(5535), pp.1647-1651.

Huang, Y., Clemens, S., Liu, W., Wang, Y. and Prell, W., 2007. Large-scale hydrological change drove the late Miocene C_4 plant expansion in the Himalayan foreland and Arabian Peninsula. *Geology*, 35(6), p.531.

Jia, G., Wei, K., Chen, F. and Peng, P., 2008. Soil *n*-alkane δD vs. altitude gradients along Mount Gongga, China. *Geochimica et Cosmochimica Acta*, 72(21), pp.5165-5174.

Jones, J., 1969. Studies on lipids of soil micro-organisms with particular reference to hydrocarbons. *Journal of General Microbiology*, 59(2), pp.145-152.

Kahmen, A., Schefuß, E. and Sachse, D., 2013a. Leaf water deuterium enrichment shapes leaf wax *n*-alkane δD values of angiosperm plants I: Experimental evidence and mechanistic insights. *Geochimica et Cosmochimica Acta*, 111, pp.39-49.

Kahmen, A., Hoffmann, B., Schefuß, E., Arndt, S., Cernusak, L., West, J. and Sachse, D., 2013b. Leaf water deuterium enrichment shapes leaf wax *n*-alkane δD values of angiosperm plants II: Observational evidence and global implications. *Geochimica et Cosmochimica Acta*, 111, pp.50-63.

Kavita, S., Guido, L.B.W., 2018. Severe drought-influenced composition and $\delta^{13}C$ of plant and soil *n*-alkanes in moderl temperate grassland and heathland ecosystems. *Organic Geochemistry*, 116, pp.77-89.

Kottek, M., Grieser, J., Beck, C., Rudolf, B., and Rubel, F., 2006. World map of the Köppen-Geiger climate classification updated. *Meteorol. Z.* **15**, pp.259–263.

Kristen, I., Wikes, H., Vieth, A., Zink, K.-G., Plessen, B., Thorpe, J., Partridge, T.C., Oberhänsli, H., 2010. Biomarker and stable carbon isotope analyses of sedimentary organic matter from Lake Tswaing: evidence for deglacial wetness and early Holocene drought from South Africa. *Journal of Paleolimnology*, 44, pp.143-160.

Kohn, M., 2010. Carbon isotope compositions of terrestrial C_3 plants as indicators of (paleo)ecology and (paleo)climate. *Proceedings of the National Academy of Sciences*, 107(46), pp.19691-19695.

Krull, E., Sachse, D., Mügler, I., Thiele, A. and Gleixner, G., 2006. Compound-specific $\delta^{13}C$ and $\delta^{2}H$ analyses of plant and soil organic matter: A preliminary assessment of the effects of vegetation change on ecosystem hydrology. *Soil Biology and Biochemistry*, 38(11), pp.3211-3221.

Kuhn, T., Krull, E., Bowater, A., Grice, K. and Gleixner, G., 2010. The occurrence of short chain *n*-alkanes with an even over odd predominance in higher plants and soils. *Organic Geochemistry*, 41(2), pp.88-95.

Lane, C.S., 2017. Modern *n*-alkane abundances and isotopic composition of vegetation in a gymnosperm-dominated ecosystem of the southeastern U.S. coastal plain. *Organic Geochemistry*, 105, pp.33-36.

Laredo, M.A., Simpson, G.D., Minson, D.J., Orpin, C.G., The potential for using *n*-alkanes in tropical forages as a marker for the determination of dry matter by grazing ruminants. *Journal of Agricultural Science*, Cambridge, 117, pp.355-361.

Li, R., Luo, G., Meyers, P.A., Gu, Y., Wang, H., Xie, S., 2012. Leaf wax *n*-alkane chemotaxonomy of bamboo from a tropical rain forest in Southwest China. *Plant Syst Evol*, 298, pp.731-738.

Li, G., Li, L., Tarozo, R., Longo, W., Wang, K., Dong, H. and Huang, Y., 2018. Microbial production of long-chain *n*-alkanes: Implication for interpreting sedimentary leaf wax signals. *Organic Geochemistry*, 115, pp.24-31.

Li, J., Huang, J., Ge, J., Huang, X., Xie, S., 2013. Chemotaxonomic significance of *n*-alkane distributions from leaf wax in genus of Sinojackia species (Styracaceae). *Biochemical Systematics and Ecology*, 49, pp.30-36.

Li, J., Tao, T., Pang, Z., Tan, M., Kong, Y., Duan, W., Zhang, Y., 2015. Identification of different moisture sources through isotopic monitoring during a storm event. *Journal of hydrometeorology*, 16, pp.1918-1927.

Liu, J.Z., Liu, W., An, Z., 2015. Insight into the reason of leaf wax δD *n*-alkane values between grasses and woods. *Science Bulletin*, 60, pp.545-555.

Liu, J.Z., Liu, W., An, Z. and Yang, H., 2016. Different hydrogen isotope fractionations during lipid formation in higher plants: Implications for paleohydrology reconstruction at a global scale. *Scientific Reports*, 6(1).

Liu, J.Z., An, Z., Wang, Z. and Wu, H., 2017. Using $\delta D_{n\text{-}alkane}$ as a proxy for paleo-environmental reconstruction: A good choice to sample at the site dominated by woods. *Science of The Total Environment*, 599-600, pp.554-559.

Liu, J.Z., An, Z. and Liu, H., 2018. Leaf wax *n*-alkane distributions across plant types in the central Chinese Loess Plateau. *Organic Geochemistry*, 125, pp.260-269.

Liu, J.Z., and An, Z., 2018. A hierarchical framework for disentangling different controls on leaf wax $\delta D_{n\text{-}alkane}$ values in terrestrial higher plants. *Quaternary Science Reviews*, 201, pp.409-417.

Liu, J.Z., and An, Z., 2019. Variations in hydrogen isotopic fractionation in higher plants and sediments across different latitudes: Implications for paleohydrological reconstruction. *Science of The Total Environment*, 650, pp.470-478.

Liu, J.Z., An, Z., Wu, H., Yu, Y., 2019. Comparison of *n*-alkane concentrations and δD values between leaves and roots in modern plants on the Chinese Loess Plateau. *Organic Geochemistry*, 138, p.103913.

Liu, J.Z., and An, Z., 2020. Leaf wax *n*-alkane carbon isotope values vary among major terrestrial plant groups: Different responses to precipitation amount and temperature, and implications for paleoenvironmental reconstruction. *Earth-Science Reviews*, 202, p.103081.

Liu, J.Z., 2021. Seasonality of the altitude effect on leaf wax *n*-alkane distributions, hydrogen and carbon isotopes along an arid transect in the Qinling Mountains. *Science of The Total Environment*, 778, p.146272.

Liu, J.Z., An, Z. and Lin, G., 2021. Intra-leaf heterogeneities of hydrogen isotope compositions in leaf water and leaf wax of monocots and dicots. *Science of The Total Environment*, 770, p.145258.

Liu, J.Z., and An, Z., 2021. Global-scale altitude effect on leaf wax *n*-alkane δD values in terrestrial higher plants. *Science China Earth Sciences*, 64(5), pp.825-834.

Liu, H., Liu, W., 2016. *n*-Alkane distributions and concentrations in algae, submerged plants and terrestrial plants from the Qinghai-Tibetan Plateau. *Organic Geochemistry*, 99, pp.10-22.

Liu, H., Yang, H., Cao, Y., Liu, W., 2018. Compound-specific δD and its hydrological and environmental implication in the lakes on the Tibetan Plateau. *Science China Earth Sciences*, 61, pp.765-777(in Chinese).

Liu, H., and Liu, W., 2019. Hydrogen isotope fractionation variations of *n*-alkanes and fatty acids in algae and submerged plants from Tibetan Plateau lakes: Implications for palaeoclimatic reconstruction. *Science of The Total Environment*, 695, pp.133925.

Liu, B., He, Y., Zhang, Y., Sun, Y., Wang, Y. and He, D., 2020. Natural and anthropogenic organic matter cycling between coastal wetlands and rivers: a case study from Liao River Delta. *Estuarine, Coastal and Shelf Science*, 236, p.106610.

Liu, W., Yang, H. and Li, L., 2006. Hydrogen isotopic compositions of *n*-alkanes from terrestrial plants correlate with their ecological life forms. *Oecologia*, 150(2), pp.330-338.

Liu, W. and Yang, H., 2008. Multiple controls for the variability of hydrogen isotopic compositions in higher plant *n*-alkanes from modern ecosystems. *Global Change Biology*, 14(9), pp.2166-2177.

Liu, W., Yang, H., Wang, H., An, Z., Wang, Z., Leng, Q., 2015. Carbon isotope composition of long chain leaf wax *n*-alkanes in lake sediments: A dual indicator of

paleoenvironment in the Qinghai-Tibet Plateau. *Organic Geochemistry*, 83-84, 190-201.

Liu, W., Wang, H., Leng, Q., Liu, H., Zhang, H., Xing, M., Cao, Y., Yang, H., 2019. Hydrogen isotopic compositions along a precipitation gradient of Chinese Loess Plateau: Critical roles of precipitation/evaporation and vegetation change as controls for leaf wax δD. *Chemical Geology,* 528, p.119278.

Liu, W.G., Yang, H., Li, L., 2006. Hydrogen isotopic compositions of *n*-alkanes from terrestrial plants correlate with their ecological life forms. *Oecologia,* 150, pp.330-338

Liu, W.G.,Yang, H.,2008. Mutiple controls for the variability of hydrogen isotopic compositions in higher plant *n*-alkane from modern ecosystems. *Global Change Biolology*, 14, pp.2166-2177.

Lockheart, M.J., Bergen, P.F. Evershed, R.P., 1997. Variations in the stable carbon isotope compositions of individual lipids from the leaves of modern angiosperms: implications for the study of higher land-derived sedimentary organic matter. *Organic Geochemistry*, 26, pp.137-153.

Luo, P., Peng, P., Gleixner, G., Zheng, Z., Pang, Z. and Ding, Z., 2011. Empirical relationship between leaf wax *n*-alkane δD and altitude in the Wuyi, Shennongjia and Tianshan Mountains, China: Implications for paleoaltimetry. *Earth and Planetary Science Letters*, 301(1-2), pp.285-296.

Luo, P., Peng, P., Lü, H., Zheng, Z. and Wang, X., 2012. Latitudinal variations of CPI values of long-chain *n*-alkanes in surface soils: Evidence for CPI as a proxy of aridity. *Science China Earth Sciences*, 55(7), pp.1134-1146.

Lütz, C., Gülz, P.G., 1985. Comparative analysis of epicuticular waxes from some high alpine plant species. *Z. Naturforsch*, 40, pp.599-605.

Maffei, M., 1994. Discriminant analysis of leaf wax alkanes in the Lamiaceae and four other plant families. *Biochemical Systematics and Ecology*, 22, pp.711-728.

Maffei, M., 1996a. Chemotaxonomic significance of leaf wax alkanes in the Gramineae. *Biochemical System&s and Ecology*, 24, pp.53-64.

Maffei, M., 1996b. Chemotaxonomic significance of leaf wax *n*-alkanes in the Umbelliferae, Cruciferae and Leguminosae (Subf. Papilionoideae). *Biochemical Systematics and Ecology*, 24, pp.531-545.

Maffei, M., Badino, S., Bossi, S., 2004, Chemotaxonomic significance of leaf wax *n*-alkanes in the Pinales (Coniferales). *Journal of Biological Research*, 1, pp.3-19.

Magill, C., Ashley, G. and Freeman, K., 2012. Ecosystem variability and early human habitats in eastern Africa. *Proceedings of the National Academy of Sciences*, 110(4), pp.1167-1174.

Malossini, F., Piasentier, E., Bovolenta, S., 1990. *n*-Alkane content of some forages. *J Sci Food Agric*, 53, pp.405-409.

Martin-Smith, M., Subramanian, G., Connor, H.E., 1967. Surface wax components of

five species of Cortaderia (Gramineae)—a chemotaxonomic comparison. *Phytochcmistry,* 6, pp.559-572.

Mayes, R.W., Beresford, N.A., Lamb, C.S., Barnett, C.L., Howard, B.J., Jones, B.E.V., Eriksson, O., Hove, K., Pedersen, Ø., Staines, B.W., 1994. Novel approaches to the estimation of intake and bioavailability of radiocaesium in ruminants grazing forested areas. The *Science of the Total Environment,* 157, pp.289-300.

Mead, R., Xu, Y., Chong, J., Jaffé, R., 2005. Sediment and soil organic matter source assessment as revealed by the molecular distribution and carbon isotopic composition of *n*-alkanes. *Organic Geochemistry,* 36, pp.363-370.

Medina, E., Aguiar, G., Go´mez, M., Ananda, J., Medina, J.D., Winter, K., 2006. Taxonomic significance of the epicuticular wax composition in species of the genus Clusia from Panama. *Biochemical Systematics and Ecology,* 34, pp.319-326.

Meyers, P. and Kites, R., 1982. Extractable organic compounds in midwest rain and snow. *Atmospheric Environment (1967)*, 16(9), pp.2169-2175.

Meyers, P., 2003. Applications of organic geochemistry to paleolimnological reconstructions: a summary of examples from the Laurentian Great Lakes. *Organic Geochemistry*, 34(2), pp.261-289.

Mimura, M.R.M., Salatino, M.L.F., Salatino, A., Baumgratz, J.F.A., 1998. Alkanes from foliar epicuticular waxes of Huberia species: taxonomic implications. *Biochemical Systematics and Ecology,* 26, pp.581-588.

Mügler, I., Sachse, D., Werner, M., Xu, B., Wu, G., Yao, T., Gleixner, G., 2008. Effect of lake evaporation on dD values of lacustrine *n*-alkanes: A comparison of Nam Co (Tibetan Plateau) and Holzmaar (Germany). *Organic Geochemistry*, 39, pp.711-729.

Nelson, D., Knohl, A., Sachse, D., Schefuß, E. and Kahmen, A., 2017. Sources and abundances of leaf waxes in aerosols in central Europe. *Geochimica et Cosmochimica Acta*, 198, pp.299-314.

Nelson, D., Ladd, S., Schubert, C. and Kahmen, A., 2018. Rapid atmospheric transport and large-scale deposition of recently synthesized plant waxes. *Geochimica et Cosmochimica Acta*, 222, pp.599-617.

Newberry, S.L., Kahmen, A., Dennis, P., Grant, A., 2015. n-Alkane biosynthetic hydrogen isotope fractionation is not constant throughout the growing season in the riparian tree Salix viminalis. *Geochimica et Cosmochimica Acta* 165, pp.75 – 85.

Nichols, J.E., Booth, R.K., Jackson, S.T., Pendall, E.G., Huang, Y., 2006. Paleohydrologic reconstruction based on *n*-alkane distributions in ombrotrophic peat. *Organic Geochemistry*, 37, pp.1505-1513.

Niedermeyer, E., Sessions, A., Feakins, S. and Mohtadi, M., 2014. Hydroclimate of the western Indo-Pacific Warm Pool during the past 24,000 years. *Proceedings of the National Academy of Sciences*, 111(26), pp.9402-9406.

Nieto-Moreno, V., Rohrmann, A., van der Meer, M., Sinninghe Damsté, J., Sachse, D., Tofelde, S., Niedermeyer, E., Strecker, M. and Mulch, A., 2016. Elevation-dependent

changes in *n*-alkane δ D and soil GDGTs across the South Central Andes. *Earth and Planetary Science Letters*, 453, pp.234-242.

Nikolić, B., Tešević, V., Đorđević, I., Jadranin, M., Todosijević, M., Bojović, S., Marin, P.D., 2010. *n*-Alkanes in the needle waxes of Pinus heldreichii var. pančići. *J. Serb. Chem. Soc.*, 75, pp.1337-1346.

Nikolić, B., Tešević, V., Đorđević, I., Todosijević, M., Mitić, Z., Bojović, S., Marin, P.D., 2020. Population diversity of *n*-alkanes in the needle cuticular wax of relicts pinus heldreichii and p. peuce from the scardopindic mountains. *Macedonian Journal of Chemistry and Chemical Engineering*, 39, pp.41–48.

Norström, E., Katrantsiotis, C., Smittenberg, R. and Kouli, K., 2017. Chemotaxonomy in some Mediterranean plants and implications for fossil biomarker records. *Geochimica et Cosmochimica Acta*, 219, pp.96-110.

Nott, C.J., Xie, S., Avsejs, L.A., Maddy, D., Chambers, F.M., Evershed, R.P., 2000. *n*-Alkane distributions in ombrotrophic mires as indicators of vegetation change related to climatic variation. *Organic Geochemistry*, 31, pp.231-235.

O'Leary, M., 1981. Carbon isotope fractionation in plants. *Phytochemistry*, 20(4), pp.553-567.

Oakes, A.M., Hren, M.T., 2016. Temporal variations in the δD of the leaf *n*-alkanes from four riparian plant species. *Organic Geochemistry*, 97, pp.122-130.

O'Connor, K.F., Berke, M.A., Ziolkowski, L.A., 2020. Hydrogen isotope fractionation

in modern plants along a boreal-tundra transect in Alaska. *Organic Geochemistry*, 147, p.104064.

Osborne, R., Salatino, M.L.F., Salatino, A., 1989. Alkanes of foliar epicuticular waxes of the genus Encephalartos. *Phytochemistry*, 28, pp.3027-3030.

Osborne, R., Salatino, A., Salatino, M.L.F., Sekiya, C.M., Torres, M.V., 1993. Alkanes of foliar epicuticular waxes from five cycad genera in the Zamiaceae. *Phytochemistry*, 33, 607-609.

Pagani, M., Pedentchouk, N., Huber, M., Sluijs, A., Schouten, S., Brinkhuis, H., Sinninghe Damsté, J. and Dickens, G., 2006. Arctic hydrology during global warming at the Palaeocene/Eocene thermal maximum. *Nature*, 442(7103), pp.671-675.

Pancost, R.D., Baasa, M., Geelc, B., Damste, J.S.S., 2002. Biomarkers as proxies for plant inputs to peats: an example from a sub-boreal ombrotrophic bog. *Organic Geochemistry*, 33, pp.675-690.

Peaple, M., Tierney, J., McGee, D., Lowenstein, T., Bhattacharya, T. and Feakins, S., 2021. Identifying plant wax inputs in lake sediments using machine learning. *Organic Geochemistry*, 156, p.104222.

Pedentchouk, N., Sumner, W., Tipple, B., Pagani, M., 2008. $\delta^{13}C$ and δD compositions of *n*-alkanes from modern angiosperms and conifers: An experimental set up in central Washington State, USA. *Organic Geochemistry*, 39, pp.1066-1071.

Pedentchouk, N. and Zhou, Y., 2018. Factors controlling carbon and hydrogen isotope

fractionation during biosynthesis of lipids by phototrophic organisms. H. Wilkes (ed.), *Hydrocarbons, Oils and Lipids: Diversity, Origin, Chemistry and Fate*, Handbook of Hydrocarbon and Lipid Microbiology.

Peterse, F., van der Meer, M., Schouten, S., Jia, G., Ossebaar, J., Blokker, J. and Sinninghe Damsté, J., 2009. Assessment of soil *n*-alkane δD and branched tetraether membrane lipid distributions as tools for paleoelevation reconstruction. *Biogeosciences*, 6(12), pp.2799-2807.

Piasentier, E., Bovolenta, S., Malossini, F., 2000. The *n*-alkane concentrations in buds and leaves of browsed broadleaf trees. *Journal of Agricultural Science,* 135, pp.311-320.

Polissar, P., Freeman, K., Rowley, D., McInerney, F. and Currie, B., 2009. Paleoaltimetry of the Tibetan Plateau from D/H ratios of lipid biomarkers. *Earth and Planetary Science Letters*, 287(1-2), pp.64-76.

Polissar, P. and Freeman, K., 2010. Effects of aridity and vegetation on plant-wax δD in modern lake sediments. *Geochimica et Cosmochimica Acta*, 74(20), pp.5785-5797.

Rao, Z., Guo, W., Cao, J., Shi, F., Jiang, H. and Li, C., 2017. Relationship between the stable carbon isotopic composition of modern plants and surface soils and climate: A global review. *Earth-Science Reviews*, 165, pp.110-119.

Reddy, C.M., Eglinton, T.I., Palic, R., Benitez-Nelson, B.C., Stojanovic G., Palic, I., Djordjevic, S., Eglinton, G., 2000, Even carbon number predominance of plant wax *n*-alkanes: a correction. *Organic Geochemistry*, 31 , pp.331-336.

Rieley, G., Collier, R., Jones, D., Eglinton, G., Eakin, P. and Fallick, A., 1991. Sources of sedimentary lipids deduced from stable carbon-isotope analyses of individual compounds. *Nature*, 352(6334), pp.425-427.

Rieley, G., Welker, J.M, Callaghan, T.V., Eglinton, G., 1995. Epicuticular waxes of two arctic species: compositional differences in relation to winter snow cover. *Phytochemistry*, 38, pp.45-52.

Rocini, C., Santos, D.Y.A.C., Graham, S., 2006. *n*-Alkane distribution patterns in species of Lythraceae sensu lato (Myrtales). *Biochemical Systematics and Ecology*, 34, pp.273-274.

Romero, I.S., Feakins, S.J., 2011. Santial gradients in plant leaf wax D/H across a coastal salt marsh in southern California. *Organic Geochemistry*, 42, pp.618-629.

Rommerskirchen, F., Plader, A., Eglinton, G., Chikaraishi, Y. and Rullkötter, J., 2006. Chemotaxonomic significance of distribution and stable carbon isotopic composition of long-chain alkanes and alkan-1-ols in C_4 grass waxes. *Organic Geochemistry*, 37(10), pp.1303-1332.

Sachse, D., Radke, J. and Gleixner, G., 2006. δD values of individual *n*-alkanes from terrestrial plants along a climatic gradient-Implications for the sedimentary biomarker record. *Organic Geochemistry*, 37(4), pp.469-483.

Sachse, D., Kahmen, A., Glexiner, G., 2009. Significant seasonal varitaion in the hydrogen isotopic composition of leaf-wax lipids for two deciduous tree ecosystems (Fagus sylvativa and Acer pseudoplatanus). *Organic Geochemistry*, 40, pp.732-742.

Sachse, D., Gleixner, G., Wilkes, H., Kahmen, A.,2010. Leaf wax *n*-alkane δD values of field-grown barley reflect leaf water δD values at the time of leaf formation. *Geochimica et Cosmochimica Acta,* 74, pp.6741-6750.

Sachse, D., Billault, I., Bowen, G., Chikaraishi, Y., Dawson, T., Feakins, S., Freeman, K., Magill, C., McInerney, F., van der Meer, M., Polissar, P., Robins, R., Sachs, J., Schmidt, H., Sessions, A., White, J., West, J. and Kahmen, A., 2012. Molecular paleoyhydrology: interpreting the hydrogen-isotopic composition of lipid biomarkers from photosynthesizing organisms. *Annual Review of Earth and Planetary Sciences*, 40(1), pp.221-249.

Sage, R., Wedin, D. and Li, M., 1999. The biogeography of C_4 photosynthesis: patterns and controlling factors. In: Sage, R. and Monson, R. (Eds.), C_4 *Plant Biology. Academic Press, San Diego, California*, pp. 313–373.

Salasoo, I., 1981. Alkane distribution in epicuticular wax of some evergreen Ericaceae. *Can. J. Bot.*, 59, pp.1188-1191.

Salasoo, I., 1983. Alkane distribution in epicuticular wax of Epacridaceae. *Phytochemistry*, 22, pp.931-942.

Salasoo, I., 1987. Epicuticular wax hydrocarbons of Ericaceae in Germany. *Z. Naturforsch*, 42, pp.499-501.

Salasoo, I., 1988. Epicuticular wax hydrocarbons of Ericaceae in the Pacific Northwest of USA. *Biochemical Systematics and Ecology,* 16, pp.619-622.

Salasoo, I., 1989a. Epicuticular wax alkanes of Ericaceae and Empetrum from alpine and sub-alpine heaths in Austria. *Plant Systematics and Evolution,* 163, pp.71-79.

Salasoo, I., 1989b. Epicuticular wax hydrocarbons of Ericaceae in British Columbia. *Biochemical Systematics and Ecology,* 17, pp.381-384.

Salatino, A., Salatino, M.L.F., Mello-silva, R.D., Duerholt-oliveira, I., 1991. An appraisal of the plasticity of alkane profiles of some species of Velloziaceae. *Biochemical Systematics and Ecology,* 19, pp.241-248.

Schefuß, E., Schouten, S., Jansen, J. and Sinninghe Damsté, J., 2003. African vegetation controlled by tropical sea surface temperatures in the mid-Pleistocene period. *Nature*, 422(6930), pp.418-421

Schefuß, E., Kuhlmann, H., Mollenhauer, G., Prange, M. and Pätzold, J., 2011. Forcing of wet phases in southeast Africa over the past 17,000 years. *Nature*, 480(7378), pp.509-512.

Schouten, S., Wolthering, M., Rijpstra, W., Sluijs, A., Brinkhuis, H. and Sinninghe Damsté, J., 2007. The Paleocene–Eocene carbon isotope excursion in higher plant organic matter: Differential fractionation of angiosperms and conifers in the Arctic. *Earth and Planetary Science Letters,* 258(3-4), pp.581-592.

Schubert, B. and Jahren, A., 2012. The effect of atmospheric CO_2 concentration on carbon isotope fractionation in C_3 land plants. *Geochimica et Cosmochimica Acta*, 96, pp.29-43.

Seki, O., Nakatsuka, T., Shibata, H. and Kawamura, K., 2010. A compound-specific *n*-alkane $\delta^{13}C$ and δD approach for assessing source and delivery processes of terrestrial organic matter within a forested watershed in northern Japan. *Geochimica et Cosmochimica Acta*, 74(2), pp.599-613.

Sessions, A.L., 2006. Seasonal changes in D/H fractionation accompanying lipid biosynthesis in Spartina alterniflora. *Geochimica et Cosmochimica Acta*, 70, pp.2153-2162.

Sessions, A.L., Burgoyne, T.W., Schimmelmann, A., Hayes, J.M., 1999. Fractionation of hydrogen isotopes in lipid biosynthesis. *Organic Geochemistry*, 30, pp. 1193-1200.

Sessions, A.L., 2016. Factors controlling the deuterium contents of sedimentary hydrocarbons. *Organic Geochemistry*, 96, pp.43-64.

Shi, M., Han, J., Wang, G., Wang, J., Han, Y., Cui, L., 2021 A long-term investigation of the variation in leaf wax *n*-alkanes responding to climate on Dongling Mountain, north China. *Quaternary International*, 592, pp.67-79.

Simoneit, B., Chester, R. and Eglinton, G., 1977. Biogenic lipids in particulates from the lower atmosphere over the eastern Atlantic. *Nature*, 267(5613), pp.682-685.

Skorupa, L., 1998. Three new species of Pilocarpus Vahl (Rutaceae) from Brazil. *Novon*, 8, pp.447-454.

Smith, F. and Freeman, K., 2006. Influence of physiology and climate on δD of leaf wax *n*-alkanes from C_3 and C_4 grasses. *Geochimica et Cosmochimica Acta*, 70(5), pp.1172-1187.

Song, X., Barbour, M., Farquhar, G., Vann, D. and Helliker, B., 2013. Transpiration rate relates to within- and across-species variations in effective path length in a leaf water model of oxygen isotope enrichment. *Plant, Cell & Environment*, 36(7), pp.1338-1351.

Sonibare1, M.A., Soladoye, M.O., Ekine-Ogunlani, Y., 2007. A chemotaxonomic approach to the alkane content of three species of Anthocleista Afzel.(Loganiaceae). *African Journal of Biotechnology,* 6, pp.1516-1520.

Sorensen, P.D., Totten, C.E., Piatak, D.M., 1978. Alkane chemotaxonomy of Arbutus. *Biochemical Systematics and Ecology,* 6, pp.109-111.

Sternberg, L., 1988. D/H ratios of environmental water recorded by D/H ratios of plant lipids. *Nature*, 333(6168), pp.59-61.

Stocker, H., Wanner, H., 1975. Changes in the composition of coffee leaf wax with development. *Phytochemistry,* 14, pp.1919-1920.

Suh, Y.J., Diefendorf, A.F., 2018. Seasonal and canopy height variation in *n*-alkanes and their carbon isotopes in a temperate forest. *Organic Geochemistry,* 116, pp.23-34.

Tipple, B.J., Ehleringer, J.R., 2018. Distinctions in heterotrophic and autotrophic-based metabolism as recorded in the hydrogen and carbon isotope ratios of normal alkanes. *Oecologia*, 187(4), pp.1053-1075.

Tipple, B., Pagani, M., Krishnan, S., Dirghangi, S., Galeotti, S., Agnini, C., Giusberti, L. and Rio, D., 2011. Coupled high-resolution marine and terrestrial records of carbon and hydrologic cycles variations during the Paleocene–Eocene Thermal Maximum (PETM). *Earth and Planetary Science Letters*, 311(1-2), pp.82-92.

Tipple, B., Berke, M., Doman, C., Khachaturyan, S., Ehleringer, J., 2013. Leaf -wax *n*-alkanes record the plant-water environment at leaf flush. *Proceeding of the National Academy of Sciecnes USA*, 110, pp.2659-2664.

Tipple, B. and Pagani, M., 2013. Environmental control on eastern broadleaf forest species' leaf wax distributions and D/H ratios. *Geochimica et Cosmochimica Acta*, 111, pp.64-77.

Tulloch, A.P., 1982. Epicuticular waxes of Panicum miliaceum, Panicum texanum and Setaria italica. *Phytochemistry*, 21, pp.2251-2255.

Tulloch, A.P., 1984. Epicuticular waxes of four Eragrostoid grasses. *Phyrockmkrry*, 23, pp.1619-1623.

Vioque, J., Pastor, J., Vioque, E., 1994, Leaf wax alkanes in the genus cozncya. *Phyrochrmurry*, 36, pp.349-352.

Vogts, A., Moossen, H., Rommerskirchen, F. and Rullkötter, J., 2009. Distribution patterns and stable carbon isotopic composition of alkanes and alkan-1-ols from plant waxes of African rain forest and savanna C3 species. *Organic Geochemistry*, 40(10), pp.1037-1054.

Vogts, A., Schefuß, E., Badewien, T. and Rullkötter, J., 2012. *n*-Alkane parameters from a deep sea sediment transect off southwest Africa reflect continental vegetation and climate conditions. *Organic Geochemistry*, 47, pp.109-119.

Wang, J., Axia, E., Xu, Y., Wang, G., Zhou, L., Jia, Y., Chen, Z., Li, J., 2018a. Temperature effect on abundance and distribution of leaf wax *n*-alkanes across a temperature gradient along the 400 mm isohyet in China. *Organic Geochemistry,* 120, pp.31-41.

Wang, J., Xu, Y., Zhou, L., Shi, M., Axia, E., Jia, Y., Chen, Z., Li, J., Wang, G., 2018b. Disentangling temperature effects on leaf wax *n*-alkane traits and carbon isotopic composition from phylogeny and precipitation. *Organic Geochemistry*, 126, pp.13-22.

Wang, Y., Larsen, T., Leduc, G., Andersen, N., Blanz, T. and Schneider, R., 2013. What does leaf wax δD from a mixed C_3/C_4 vegetation region tell us? *Geochimica et Cosmochimica Acta*, 111, pp.128-139.

Wang, Z. and Liu, W., 2012. Carbon chain length distribution in *n*-alkyl lipids: A process for evaluating source inputs to Lake Qinghai. *Organic Geochemistry*, 50, pp.36-43.

Wang, Z., Liu, H. and Cao, Y., 2018. Choosing a suitable $\varepsilon_{w\text{-}p}$ by distinguishing the dominant plant sources in sediment records using a new P_{ta} index and estimating the paleo-δD_p spatial distribution in China. *Organic Geochemistry,* 121, pp.161-168.

Wang, Z., Liu, W., Wang, H., Cao, Y., Hu, J., Dong, J., Lu, H., Wang, H., Xing, M. and Liu, H., 2021. New chronology of the Chinese loess-paleosol sequence by leaf wax δD records during the past 800 k.y. Geology, 49 (7). DOI: 10.1130/G48833.1.

Wannigama, G.P., Volkman, J.K., Gillan, F.T., Nichols, P.D., Johns, R.B., 1981. A comparison of lipid components of the fresh and dead leaves and pneumatophores of the mangrove Avicennia marina. *Phytochemistry*, 20, pp.659-666.

Wen, R., Xiao, J., Fan, J., Zhang, S. and Yamagata, H., 2017. Pollen evidence for a mid-Holocene East Asian summer monsoon maximum in northern China. *Quaternary Science Reviews*, 176, pp.29-35.

Wu, M., Feakins, S., Martin, R., Shenkin, A., Bentley, L., Blonder, B., Salinas, N., Asner, G. and Malhi, Y., 2017. Altitude effect on leaf wax carbon isotopic composition in humid tropical forests. *Geochimica et Cosmochimica Acta,* 206, pp.1-17.

Xie, S., Nott, C.J., Avsejs, L.A., Maddy, D., Chambers, F.M., Evershed, R.P., 2004, Molecular and isotopic stratigraphy in an ombrotrophic mire for paleoclimate reconstruction. *Geochimica et Cosmochimica Acta*, 68, pp.2849-2862.

Yan, C, Zhang, Y, Zhang, Y, Zhang, Z, Huang, X, 2020. Habitat influence on the Molecular, carbon and hydrogen isotope compositions of leaf wax *n*-alkanes in a

subalpine basin, central China. *Journal of Earth Science,* 31, pp.845-852.

Yang, H., Huang, Y., 2003. Preservation of lipid hydrogen isotope ratios in Miocene lacustrine sediments and plant fossils at Clarkia, northern Idaho, USA. *Organic Geochemistry,* 34, pp.413-423.

Yang, H., Blais, B., Leng, Q., 2011a. Stable isotope variations from cultivated Metasequoia trees in the United States: A statistical approach to assess isotope signatures as climate signals. *Japanese Journal of History Botany,* 19, pp.75-88.

Yang, H., Liu, W.G., Leng, Q., Hren, M.T., Pagani, M.,2011b. Variation in *n*-alkane δD values from terrestrial plants at high latitude: Implications for paleoclimate reconstruction. *Organic Geochemistry,* 42, pp.283-288.

Yao, L., Guo, N., He, Y., Xiao, Y., Li, Y., Gao, J., Guo, Y., 2021. Variations of soil organic matters and plant cuticular waxes along an altitude gradient in Qinghai-Tibet Plateau. *Plant and Soil*, 458, pp.41-58.

Zhang, Y., Togamura, Y., Otsuki, K., 2004. Study on the *n*-alkane patterns in some grasses and factors affecting the *n*-alkane patterns. *Journal of Agricultural Science*, 142, pp.469-475.

Zhang, X., Xu, B., Günther, F., Mügler, I., Lange, M., Zhao, H., Li, J. and Gleixner, G., 2017. Hydrogen isotope ratios of terrestrial leaf wax *n*-alkanes from the Tibetan Plateau: Controls on apparent enrichment factors, effect of vapor sources and implication for altimetry. *Geochimica et Cosmochimica Acta*, 211, pp.10-27.

Zhao, B., Zhang, Y., Huang, X., Qiu, R., Zhang, Z., Meyers, P.A., 2018. Comparison of *n*-alkane molecular, carbon and hydrogen isotope compositions of different types of plants in the Dajiuhu peatland, central China. *Organic Geochemistry,* 124, pp.1-11.

Zhuang, G., Brandon, M., Pagani, M. and Krishnan, S., 2014. Leaf wax stable isotopes from Northern Tibetan Plateau: Implications for uplift and climate since 15 Ma. *Earth and Planetary Science Letters*, 390, pp.186-198.

Zygadlo, J.A., Abburra, R.E., Maestri, D.M., Guzman, C.A., 1992. Distribution of alanes and fatty acids in the Condalia montana (Rhamnaceae) species complex. *Plant Systematics and Evolution,* 179, pp.89-93.

Zygadlo, J.A., Maestri, D.M., Grosso, N.R., 1994. Alkane distribution in epicuticular waxes of some Solanaceae species. *Biochemical Systematics and Ecology,* 22, pp.203-209.

Figure captions

Fig. 1 Global maps showing the site distributions of terrestrial leaf wax biomarkers (*n*-alkanes, a; δ^2H_{wax}, b; $\delta^{13}C_{wax}$, c); Proportions of *n*-alkane distributions (ACL, d; CPI, e), δ^2H_{wax} (f), and $\delta^{13}C_{wax}$ (c) across different plant types (woods vs. non-woods for n-alkanes, dicots vs. monocots for δ^2H_{wax}, and C_3 vs. C_4 for $\delta^{13}C_{wax}$). Global distribution of the Köppen–Geiger climate classification. The black dots are data from prior datasets, and red dots are additional data points.

Fig. 2 Average long-chain *n*-alkane distributions (C_{27}-C_{35}) across plant life forms (e.g., tree, shrub, herb, forb, grass, sedge; a), taxonomic lineages (e.g., dicot, monocot,

gymnosperm, magnoliid, b), and wood vs. non-wood (c) in terrestrial higher plants. The new *n*-alkane dataset (n = 3365) was expanded based upon the previous dataset of Bush and McInerney (2013). The *n*-alkane data were from Ali et al., 2005a, b; Avato et al., 1984; Badewien et al., 2015; Bezabih et al., 2010; Bojović et al., 2012; Bugalho et al., 2004; Bush and McInerney., 2013; Bush and McInerney., 2015; Carr et al., 2014; Castillo et al., 1967; Cerda-Peña et al., 2020; Chen et al., 1998; Cifuentes et al., 2020; Diefendorf et al., 2015; Dion-Kirschner et al., 2020; Dodoš et al., 2015; Dove H., 1992; Dove and Mayes., 2005; Duan et al., 2016; Eglinton et al., 1962; Feakins et al., 2016b; Feakins and Sessions., 2010a, b; Ficken et al., 1998; Gamarra and Kahmen., 2015; Gülz et al., 1989; Guo et al., 2016; Guo et al., 2014; Guo et al., 2015; Hall et al., 1965; Herbin and Robins., 1968a, b; Herbin and Robins., 1969; Horn et al., 1964; Howard et al., 2018; Lane C.S., 2017; Laredo et al., 1991; Li et al., 2013; Li et al., 2012; Liu et al., 2018; Liu et al., 2019; Lütz and Gülz., 1985; Maffei M., 1994; Maffei et al., 2004; Maffei M., 1996a, b; Malossini et al., 1990; Martin-Smith et al., 1967; Mayes et al., 1994; Medina et al., 2006; Mimura et al., 1998; Nichols et al., 2006; Nikolić et al., 2010; Nikolić et al., 2020; Nott et al., 2000; Oakes and Hren., 2016; O'Connor et al., 2020; Osborne et al., 1993; Osborne et al., 1989; Pancost et al., 2002; Piasentier et al., 2000; Reddy et al., 2000; Rieley et al., 1995; Rocini et al., 2006; Rommerskirchen et al., 2006; Sachse et al., 2009; Salasoo L., 1981; Salasoo L., 1983; Salasoo L., 1987; Salasoo L., 1989, b; Salasoo L., 1988; Salatino L., 1991; Shi et al., 2021; Skorupa L., 1998; Smith et al., 2006; Sonibare1 and Freeman., 2007; Sorensen et al., 1978; Stocker and Wanner., 1975; Tipple and Ehleringer., 2018; Tulloch A.P., 1982; Tulloch A.P., 1984; Vioque et al., 1994; Vogts et al., 2009; Wang et al., 2018a; Wannigama et al., 1981; Xie et al., 2004; Yan et al., 2020; Yao et al., 2021; Zhang et al., 2004; Zygadlo et al., 1994; Zygadlo et al., 1992.

Fig. 3 Boxplots for the differences in terrestrial leaf wax *n*-alkane indices such as ACL (average chain length), CPI (carbon preference index), $C_{29}/(C_{29} + C_{31})$, and $(C_{27} + C_{29})/(C_{27} + C_{29} + C_{31} + C_{33})$ among life forms (a, b, c, d), plant types (e, f, g, h), and wood vs. non-wood (I, j, k, l).

Fig. 4 Differences in the typical *n*-alkane indices such as ACL and CPI between wood and non-wood across five climate zones, and along latitude and longitude gradients.

Fig. 5 Evolution of the effect of plant types on δ^2H_{wax} values in terrestrial higher plants, especially at scale transitions. (a) photosynthetic pathways (e.g., Chikaraishi and Naraoka, 2003); (b) plant life forms (grasses vs. woods) at a catchment scale (Liu et al., 2006); (c) plant life forms at the global scale (Liu and Yang, 2008); (d) plant taxonomic lineages (dicots vs. monocots) at the global scale (Liu et al., 2016) and catchment scale (Liu et al., 2017). This figure was modified from Liu and An (2018).

Fig. 6 Differences in δ^2H_{wax} values between dicots and monocots across climate zones over the globe. The global map was from the global distribution of the Köppen–Geiger climate classification. The δ^2H_{wax} data were from Bai et al., 2011; Bai et al., 2014; Bai et al., 2019; Bai et al., 2020; Balascio et al., 2018; Berke et al., 2019; Bi et al., 2005; Chikaraishi and Naraoka, 2003; Daniels et al., 2017; Dion-Kirschner et al., 2020; Duan et al., 2010; Duan et al., 2011a, b; Duan et al., 2014; Duan et al., 2018.; Eley et al., 2014; Feakins and Sessions, 2010a; Feakins et al., 2016; Freimuth et al., 2017; Freimuth et al., 2019; Gao et al., 2014b; Griepentrog et al., 2019; He et al., 2020; Hou et al., 2007; Kahmen et al., 2013b; Krull et al., 2006; Liu and Liu, 2016; Liu and Yang, 2008; Liu et al., 2006; Liu et al., 2015; Liu et al., 2017; Liu et al., 2018; Liu et al., 2019; Mügler et al., 2008; Oake and Hren, 2016; O'Connor et al., 2020; Pedenchouk et al., 2008, Romero and Feakins, 2011; Sachse et al., 2006; Sachse et al., 2009; Sachse et al., 2010; Sessions, 2006; Smith and Freeman, 2006; Tipple et al., 2013; Tipple and Pagani, 2013; Wang et al., 2018; Yan et al., 2020; Yang and Huang, 2003; Yang et al., 2011a, b; Zhang et al., 2017; Zhao et al., 2018.

Fig. 7 Variations of δ^2H_{wax} values and apparent fractionation ε_{app} values in terrestrial higher plants. Significant increases in δ^2H_{wax} values vary with δ^2H_p values between dicots and monocots, but no or weak correlations occur in ε_{app} values with δ^2H_p values in dicots and monocots (a, c). Boxplots for δ^2H_{wax} and ε_{app} values between dicots and monocots (b, d).

Fig. 8 Statistical analysis of global $\delta^{13}C_{wax}$ values in terrestrial higher plants. Boxplot for plant types separated by major taxonomic group and photosynthetic pathways (a).

The $\delta^{13}C_{wax}$ values distributed across plant taxonomic lineages at the family level (the red shadow indicates C_3 plants, and the blue shadow means C_4 plants; b). The $\delta^{13}C_{wax}$ data were from Ankit et al., 2017; Badewien et al., 2015; Bezabih et al., 2011; Bi et al., 2005; Boom et al., 2014; Ceccopieri et al., 2021; Chikaraishi and Naraoka, 2003; Chikaraishi and Naraoka, 2006; Chikaraishi et al., 2004; Collister et al., 1994; Conte et al., 2003; Diefendorf et al., 2011; Diefendorf et al., 2015; Dion-Kirschner et al., 2020; Duan and He, 2011; Eley et al., 2016; Garcin et al., 2014; Ho et al., 2015; Hockun et al., 2016; Kristen et al., 2010; Krull et al., 2006; Lane, 2017; Liu et al., 2015; Liu J.Z., 2021; Lockheart et al., 1997; Mead et al., 2005, Rommerskirchen et al., 2006; Srivastava and Wiesenberg, 2018; Suh and Diefendorf, 2018; Vogts et al., 2009; Wang et al., 2018b; Wu et al., 2017; Yan et al., 2020; Zhao et al., 2018.

Fig. 9 Differences in $\delta^{13}C_{wax}$ values between C_3 and C_4 plants across climate zones. The global average $\delta^{13}C_{wax}$ values were 35.6±5.2 and -21.9±2.4 for C_3 and C_4 plants, respectively. The global map was from the global distribution of the Köppen–Geiger climate classification.

Fig. 10 Linear correlations between $\delta^{13}C_{wax}$ values of C_3 and C_4 plants and MAP (mean annual precipitation; a) and MAT (mean annual temperature; b). The mechanism for explaining different responses of $\delta^{13}C_{wax}$ values of C_3 and C_4 plants to precipitation amount and temperature. The shaded area represents 95% confidence level. The figure was modified from Liu and An (2020).

Fig. 11 The effects of plan types, three forms of expression (non-wood vs. wood, dicot vs. monocot, C_3 vs. C_4), on leaf wax *n*-alkane biomarkers (*n*-alkane distributions, $\delta^{2}H_{wax}$ and $\delta^{13}C_{wax}$ values) in terrestrial plants.

Fig. 12 Conceptual model of relationship effect of plant types and other factors on leaf wax biomarkers. The effects of plant types on three forms of leaf wax biomarkers (wood vs. non-wood for *n*-alkanes, dicot vs. monocot for $\delta^{2}H_{wax}$, and C_3 vs. C_4 for $\delta^{13}C_{wax}$). The coupled proxies of leaf wax biomarkers can be effectively used to reduce errors and uncertainties in paleohydroclimates, paleovegetation, and paleoaltitude reconstructions.

Fig. 13 Applications of Terrestrial leaf wax biomarkers to paleoclimate and paleovegetation. (a) Average chain length (ACL) and the $C_{31}/(C_{29} + C_{31})$ *n*-alkane ratio records at MD96-2048 over the past 800 ka, indicating the change in the proportion of grassland and forest in the southern East African (Castañeda et al., 2016). (b) The $\delta^{13}C_{wax}$ records at ODP Site 1077 and African C_4 plant abundance reconstructions between 1.2 and 0.45 million years ago (Schefuß et al., 2003). (c) The $\delta^{2}H_{wax}$ records at ODP Site 722 in the Arabian Sea, reflecting hydrological changes over past 11 million years in Himalayan foreland and Arabian Peninsula (Huang et al., 2007). (d) The $\delta^{13}C_{wax}$ and $\delta^{2}H_{wax}$ records in Lake Laguna La Gaiba and vegetation-normalized $\delta^{2}H_{wax}$ values calibrated by $\delta^{13}C_{wax}$-$\delta^{2}H_{wax}$ relationship (Fornace et al., 2016).

Abstract

Terrestrial leaf wax *n*-alkane biomarkers provide considerable insights into paleoenvironmental reconstruction. Over decades, a substantial number of field investigations were performed to constrain hydroclimatic factors that influence leaf wax *n*-alkane biomarkers to improve their utility for paleoenvironmental applications. However, a critical issue, the plant type effects, does exist which potentially affects the fidelity of leaf wax *n*-alkane biomarkers for paleohydroclimate calibration. Here we review the effects of plant types on terrestrial leaf wax *n*-alkane biomarkers from three aspects: leaf wax *n*-alkane distribution (wood vs. non-wood), hydrogen isotope (δ^2H_{wax}; dicot vs. monocot) and carbon isotope ($\delta^{13}C_{wax}$; C_3 vs. C_4) biomarkers. Then we demonstrate the relationships between three forms of leaf wax *n*-alkane biomarkers, and provide examples of the cross-calibration among them in paleo-applications. The in-depth review of plant type effects on leaf wax *n*-alkane biomarkers will be helpful to interpret the hydroclimate and vegetation signals in the geologic past.

Competing interests

The authors declare that they have no known competing financial interests or personal relationships that could have appeared to influence the work reported in this paper.

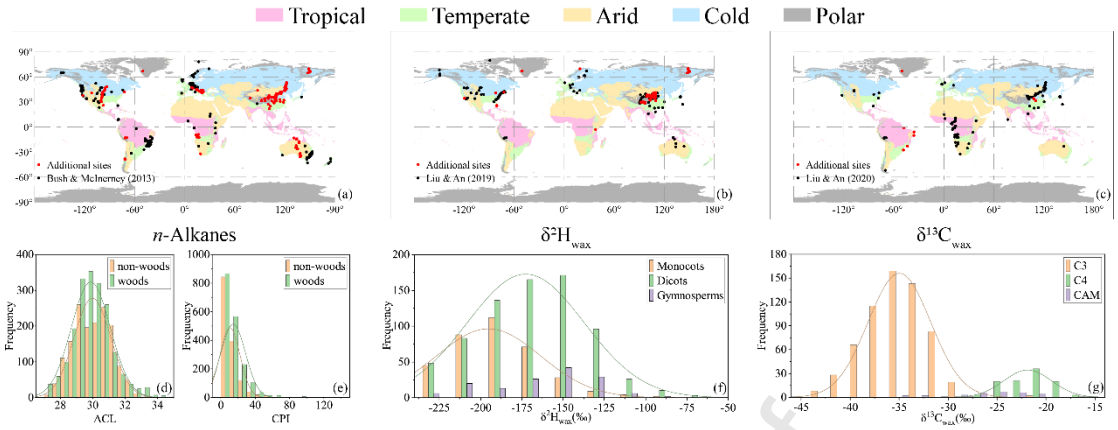

Figure-1

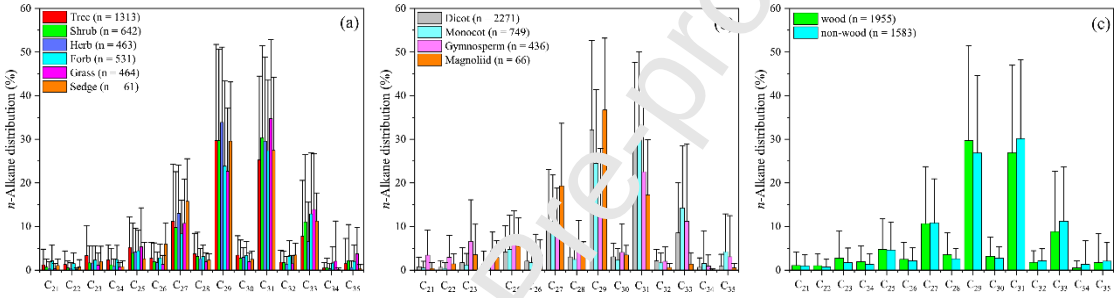

Figure-2

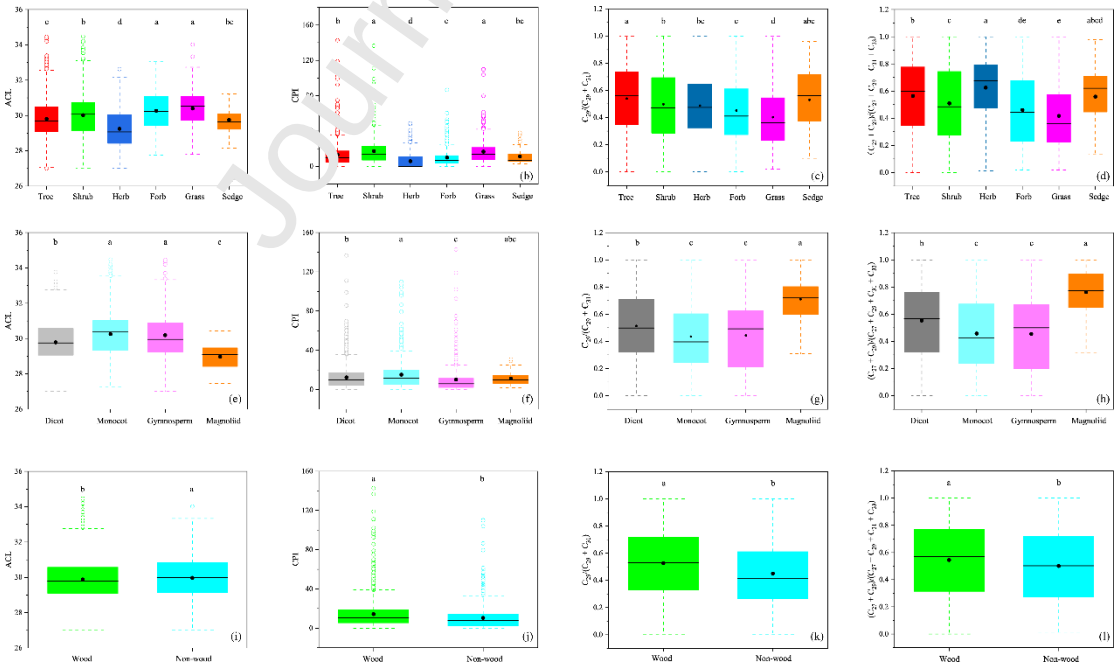

Figure-3

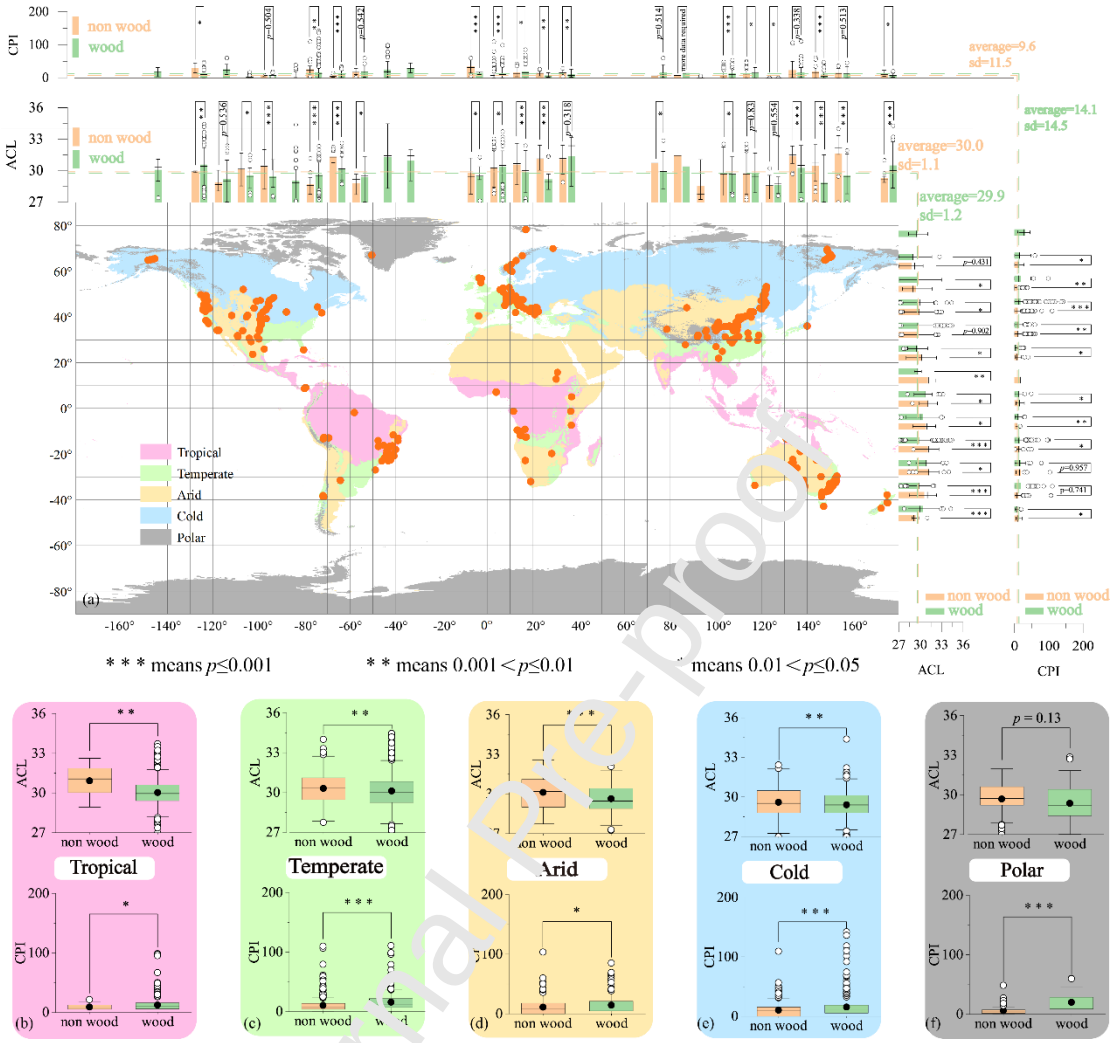

Figure-4

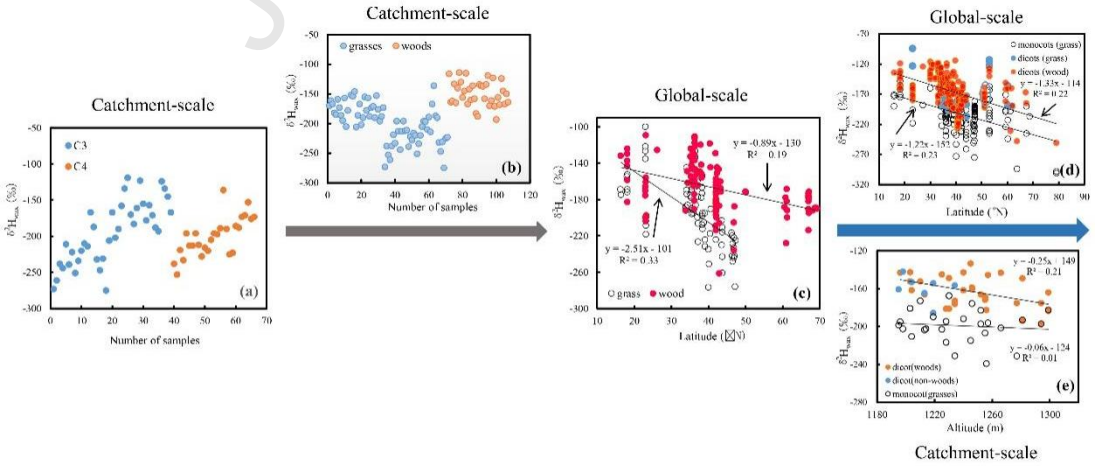

Figure-5

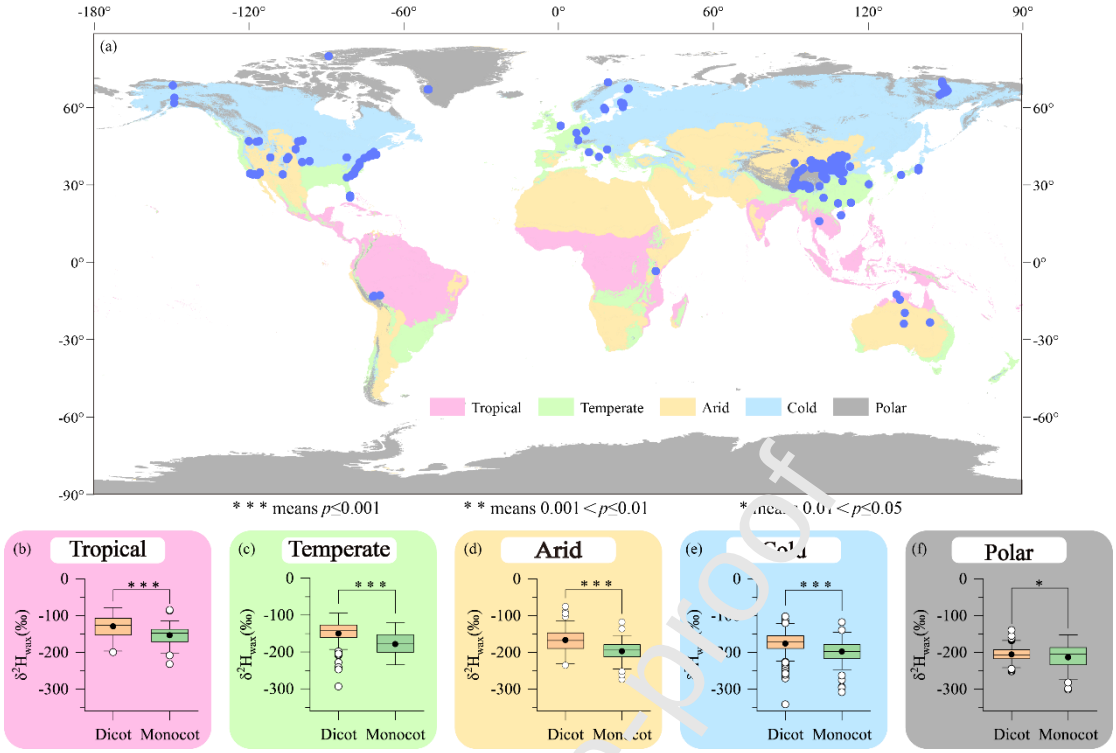

Figure-6

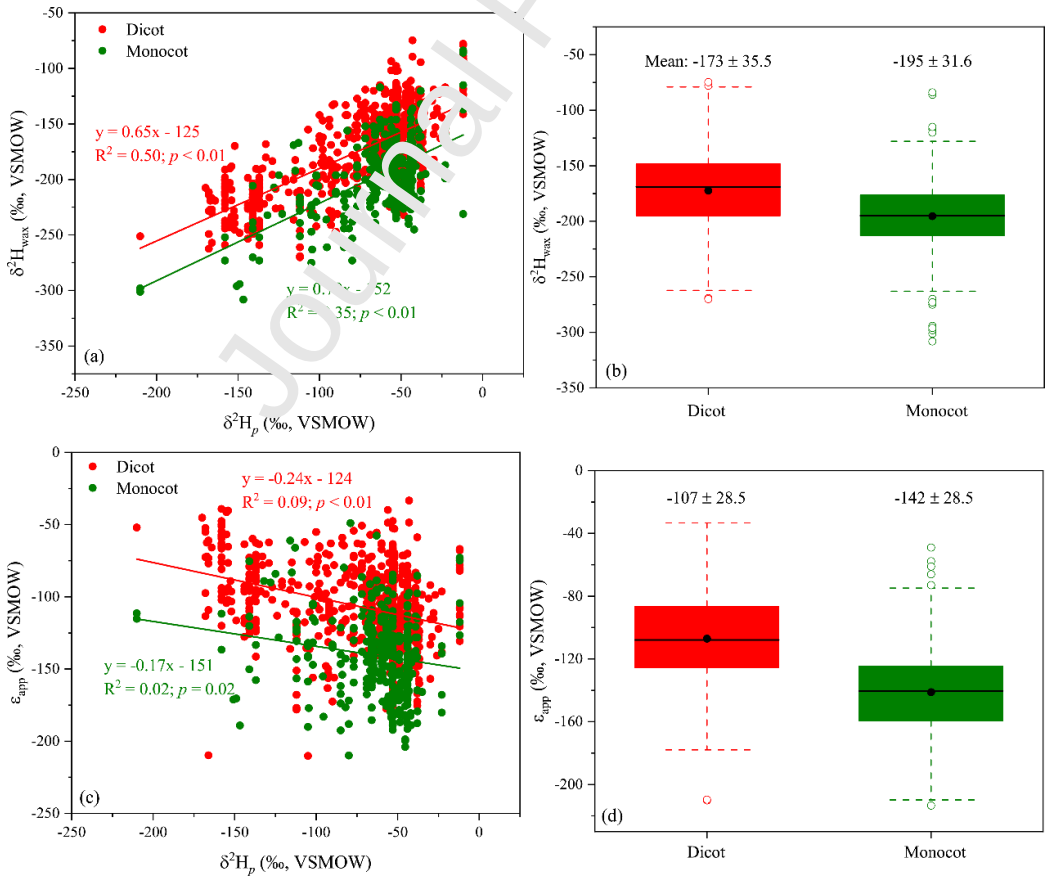

Figure-7

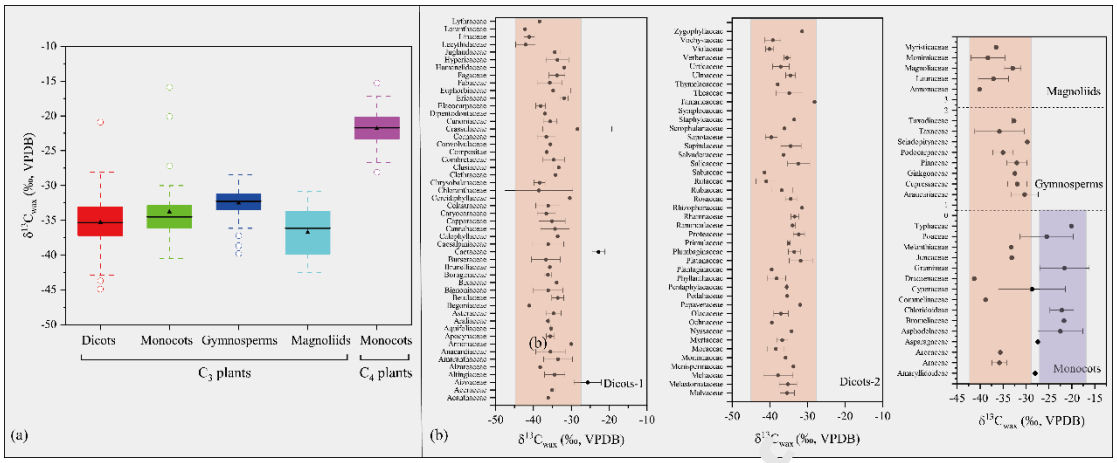

Figure-8

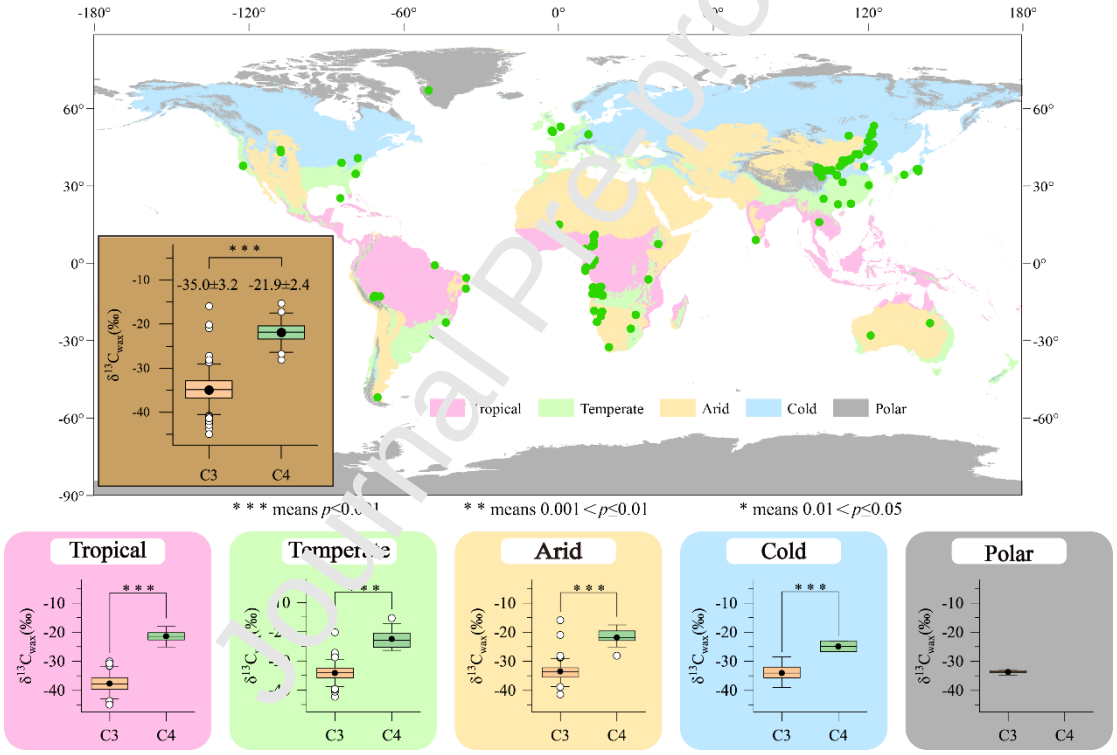

Figure-9

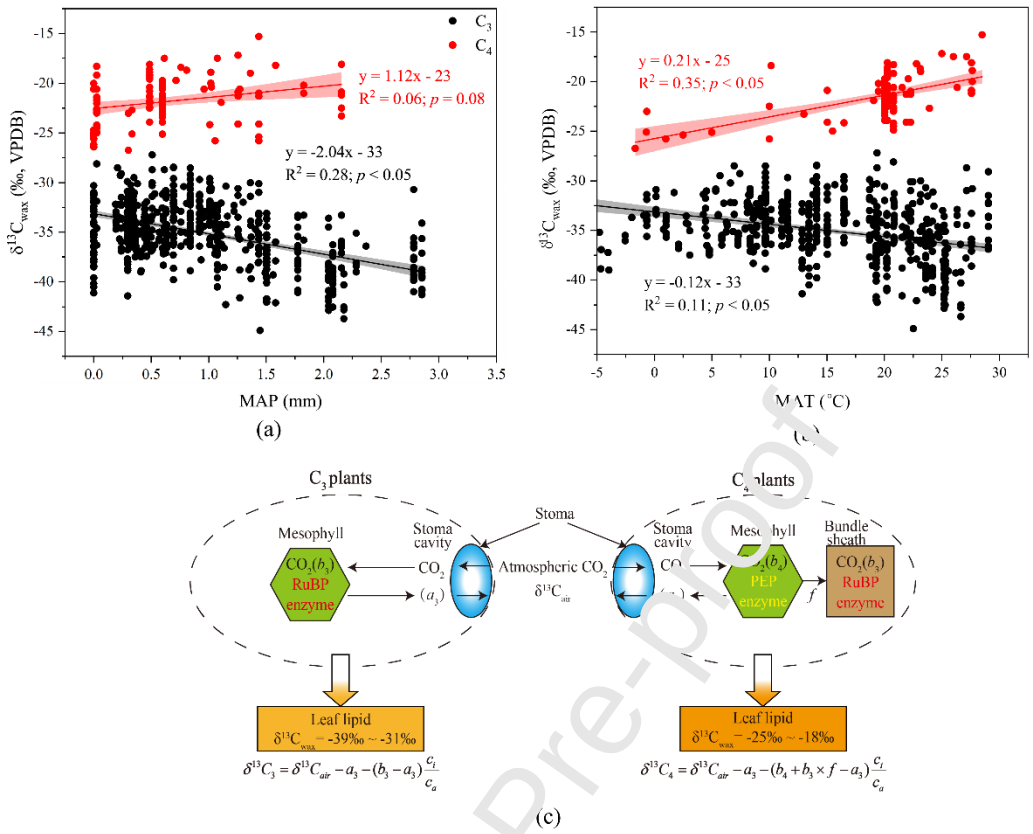

Figure-10

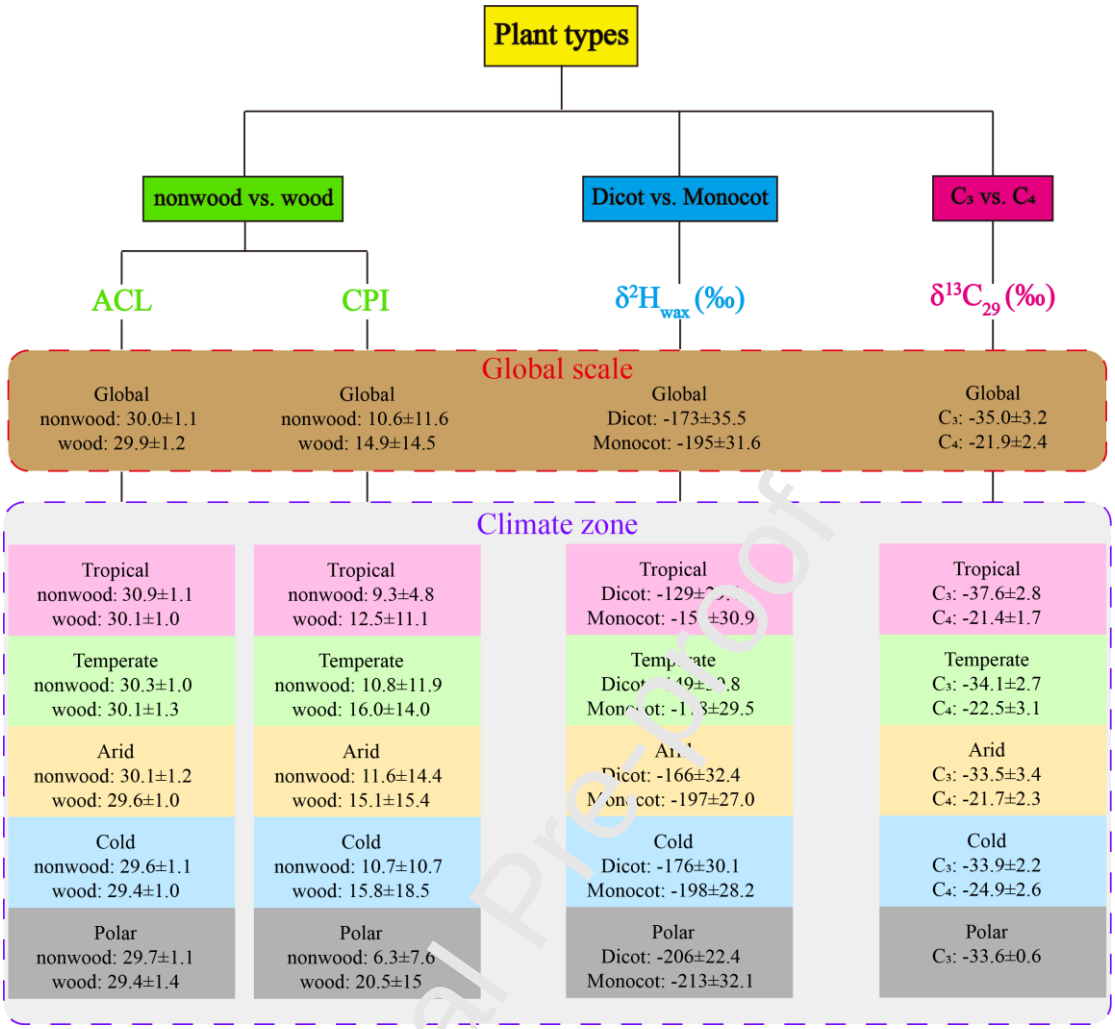

Figure-11

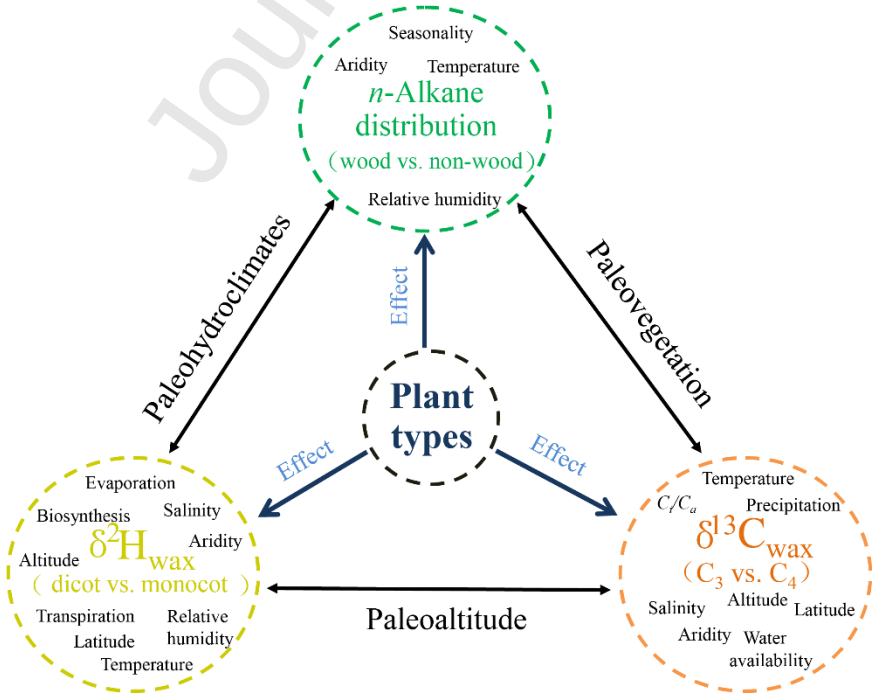

Figure-12

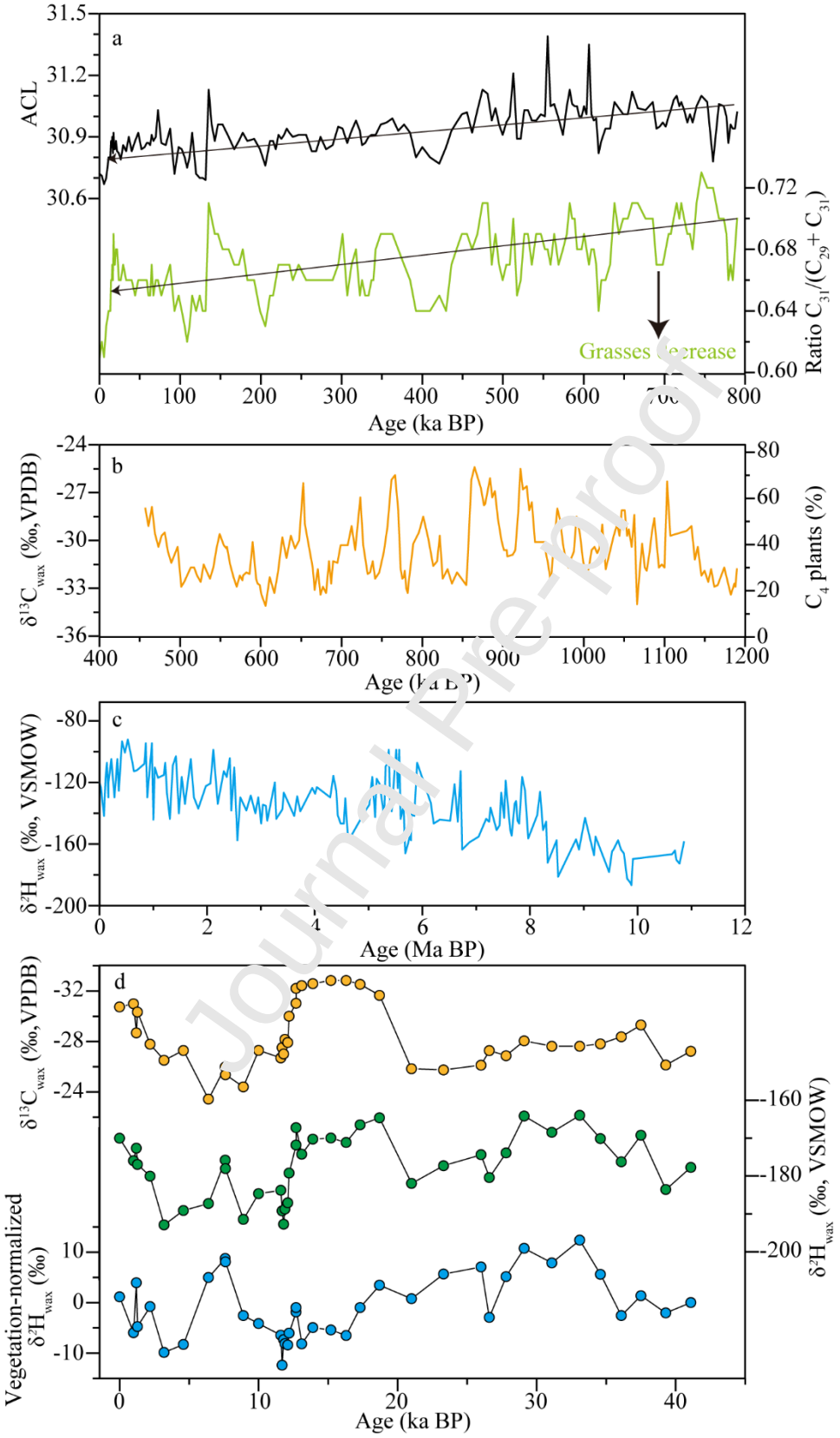

Figure-13